

# Off-shell effects in the electromagnetic production of strangeness

T. Mizutani<sup>1</sup>, C. Fayard<sup>2</sup>, G.-H. Lamot<sup>2</sup>, and B. Saghai<sup>3</sup>

1) *Department of Physics, Virginia Polytechnic Institute and State University  
Blacksburg, VA 24061 USA*

2) *Institut de Physique Nucléaire de Lyon, IN2P3-CNRS, Université Claude Bernard,  
F-69622 Villeurbanne Cedex, France*

3) *Service de Physique Nucléaire, CEA-Saclay, F-91191 Gif-sur-Yvette, France*  
(September 21, 2018)

## Abstract

Previous approaches to the photo- and electro-production of strangeness off the proton, based upon effective hadronic Lagrangians, are extended here to incorporate the so called *off-shell effects* inherent to the fermions with spin  $\geq 3/2$ . A formalism for intermediate-state, spin  $3/2$ , nucleonic and hyperonic resonances is presented and applied to the processes  $\gamma p \rightarrow K^+\Lambda$ , for  $E_\gamma^{lab} \leq 2.5$  GeV,  $ep \rightarrow e'K^+\Lambda$ , as well as the branching ratio for the crossed channel reaction  $K^-p \rightarrow \gamma\Lambda$ , with stopped kaons. The sensitivity, from moderate to significant, of various observables to such effects are discussed.

PACS: 25.20.Lj, 25.30.Rw, 13.88.+e, 13.60.-r

## I. INTRODUCTION

The purpose of the present work is to improve the recent Saclay-Lyon (SL) study [1] on the strangeness electromagnetic production from the proton. This latter investigation was based upon an effective hadronic Lagrangian in the lowest (tree) approximation, often called the isobar approximation. In a number of aspects one might safely say that SL is an improved version of its predecessors dealing with the same strangeness production processes<sup>1</sup>. In particular, it has incorporated the  $s$ -channel nucleonic resonances with spin  $3/2$  and  $5/2$ , expected to be important should the model keep adequate as energy increases. In Ref. [2] such resonances were also considered. However, there the components of the amplitude growing undesirably with increasing channel energy were taken away by hand.

As we will see later, these contributions arise from the non-resonant terms associated to each considered resonance with spin  $> 1/2$ . In the SL study this was avoided by modifying the vertices and propagators in a manner adopted for spin  $3/2$  resonances in Refs. [3,4]: a straightforward extension to higher spins, while preserving the electromagnetic gauge invariance.

This modification, however, has introduced an unwanted behavior for spin  $> 1/2$  hyperonic resonances exchanged in the  $u$ -channel: the corresponding propagators become singular in the physical region. Thus in the SL approach only spin  $1/2$  hyperons have been considered in the  $u$ -channel exchange. The phenomenological success of the SL model might imply that, within the present state of the data, the main contributions from baryonic higher spin resonances come mainly from the  $s$ -channel resonances (we will come back to this point in section IV).

In the study of pion photoproduction, the Rensselaer Polytechnic Institute (RPI) group [5,6] has shown that of several different forms of the spin  $3/2$  propagator in the literature only one of them has a correct inverse. Also the authors pointed out that there are extra degrees of freedom associated with the interaction vertices involving a spin  $3/2$  particle. By exploiting these facts, they successfully fitted the existing photo-pion data by the amplitudes generated from effective hadronic Lagrangians, and made predictions for some observables as well as the  $E2/M1$  ratio for the  $N\Delta\gamma$  vertex. A similar strategy has been applied also by the RPI group [7,8] to the photo- and electro-production of the  $\eta$  meson.

---

<sup>1</sup> See Ref. [1] for a detailed account on this matter and extensive references to relevant papers.

It seems quite natural then, as an extension of the Saclay-Lyon approach [1], as well as the works of the RPI group [5–8], to exploit this treatment for spin 3/2 particles in the study of the photo- and electro-production of the strangeness off the nucleon. Yet, one needs to incorporate properly the  $u$ -channel exchanges in the phenomenological approaches. The reasons for such an effort are mainly two-fold: (i) a consistent treatment of the higher spin baryonic resonances in both  $s$ - and  $u$ -channels, (ii) very likely, more sophisticated formalisms will be needed to interpret the forthcoming data from new facilities, *e.g.*, the Thomas Jefferson National Accelerator Facility (JLAB), the Electron Stretcher Accelerator (ELSA), the European Synchrotron Radiation Facility (ESRF), and the 8 GeV Synchrotron facility (SPRING-8) under construction in Japan.

In this paper, we work out the general expressions valid for the processes with a kaon  $K$  ( $\equiv K^+, K^0$ ) and an hyperon  $Y$  ( $\equiv \Lambda, \Sigma^0, \Sigma^+$ ) in the final state. A selected set of  $K\Lambda$  channel observables for the following processes are also reported:  $\gamma p \rightarrow K^+\Lambda$  ( $E_\gamma^{lab} \leq 2.5$  GeV),  $ep \rightarrow e'K^+\Lambda$ , and  $K^-p \rightarrow \gamma\Lambda$ . Similar investigations with the  $\Sigma$  hyperons in the final state, *i.e.*  $K^+\Sigma^0$  and  $K^0\Sigma^+$  channels, are in progress and the results will be reported elsewhere.

In section II, the approach by the RPI group is extended to the photo- and electroproduction of strangeness through  $s$ -channel nucleonic resonances of spin 3/2. The off-shell parameters are introduced in the interaction Lagrangians, and the dependence on these parameters of the non-pole part of the invariant amplitudes is clarified. The approaches used previously where the off-shell effects were ignored are placed in the present context. Section III is devoted to the treatment of spin 3/2 resonances in the  $u$ -channel. The direct calculation proceeds along the same line as for the  $s$ -channel resonance exchange. The substitution rule which emerges from the direct calculation is worked out, leading to simple rules to obtain the  $u$ -channel invariant amplitudes from the  $s$ -channel ones. In section IV, we give our results and we discuss the dependence of the relevant observables on the off-shell parameters. The summary and conclusions are presented in the last section.

## II. SPIN 3/2 RESONANCES IN THE $S$ -CHANNEL

In this section we extend the approach by Benmerrouche *et al.* [5–7], devoted to the  $\pi$  and  $\eta$  photoproduction, to obtain the amplitudes for the reactions  $\gamma_{R,V}p \rightarrow KY$  ( $KY \equiv K^+\Lambda, K^+\Sigma^0, K^0\Sigma^+$ ) for both real ( $\gamma_R$ ) and virtual ( $\gamma_V$ ) photons, through an  $s$ -channel nucleonic resonance of spin 3/2 and positive parity. Once we obtain the amplitude, it is easy to establish its relation to the corresponding one obtained by Renard & Renard [2] as well as to the one in SL [1]. Also one finds that the amplitudes due to nucleonic  $s$ -channel  $3/2^-$  resonances may be trivially obtained by simple substitutions. Although some parts of this section should appear to be repetitive to those who are familiar with Ref. [5], we give a comprehensive presentation of the matter for completeness, and present the explicit expressions of the invariant amplitudes for the photo- and electro-production.

### A. Free Lagrangian

We first define<sup>2</sup> the nucleon field as  $N$  and a spin 3/2 (isospin 1/2) vector spin field (resonance) as  $R^\mu$ . Then the free Lagrangian for the spin 3/2 field reads

$$\mathcal{L}_{free} = \bar{R}^\alpha \Lambda_{\alpha\beta} R^\beta, \quad (2.1)$$

where  $\bar{R}^\alpha$  is the usual Dirac conjugate of  $R^\alpha$ , and

$$\Lambda_{\alpha\beta} = -[(-i\not{\partial} + M_R)g_{\alpha\beta} - iA(\gamma_\alpha\not{\partial}_\beta + \gamma_\beta\not{\partial}_\alpha) - \frac{i}{2}(3A^2 + 2A + 1)\gamma_\alpha\not{\partial}\gamma_\beta - M_R(3A^2 + 3A + 1)\gamma_\alpha\gamma_\beta], \quad (2.2)$$

with  $M_R$  the mass of the resonance, and  $A(\neq -1/2)$  being a free parameter which preserves the invariance of the physical quantities constructed from the field under the point transformation

$$R^\mu \rightarrow R^\mu + a\gamma^\mu\gamma^\nu R_\nu, \quad (2.3)$$

$$A \rightarrow A + (A - 2a)/(1 + 4a), \quad (2.4)$$

$a \neq -1/4$ , but otherwise arbitrary. The free spin 3/2 field satisfies the equation of motion and two constraints

---

<sup>2</sup> Throughout the present article we follow the conventions found in Bjorken and Drell [9].

$$(i\rlap{-}\not{\partial} - M_R)R^\mu = 0, \quad (2.5)$$

$$\gamma_\mu R^\mu = 0, \quad (2.6)$$

$$\partial_\mu R^\mu = 0. \quad (2.7)$$

The above constraints ensure that  $R$  has spin 3/2 with upper (positive energy) and lower (negative energy) components.

The propagator associated with the  $R$  field is obtained from the equation

$$\Lambda_{\alpha\beta}P_\delta^\beta = g_{\alpha\delta}. \quad (2.8)$$

We may set  $A = -1$  to find the simplest form for the propagator

$$P_{\mu\nu}(q) = \frac{\not{q} + M_R}{3(q^2 - M_R^2)} \left[ 3g_{\mu\nu} - \gamma_\mu\gamma_\nu - \frac{2q_\mu q_\nu}{M_R^2} - \frac{q_\nu\gamma_\mu - q_\mu\gamma_\nu}{M_R} \right], \quad (2.9)$$

where  $q$  is the four momentum of the resonance. It is important to note [5] that this propagator contains the spin 1/2 contribution, which is a consequence of the fact that the above  $P^{\mu\nu}$  has the correct inverse.

## B. Interaction Lagrangians

Now we introduce the interactions for  $\gamma_{R,\nu}p \rightarrow KY$  through the  $s$ -channel spin 3/2 resonance discussed above. Again following Ref. [5] with some modifications appropriate for the processes under consideration, the most general interaction Lagrangian which preserves the symmetry under the point interaction introduced in the previous Subsection reads

$$\mathcal{L}_{KYR} = \frac{g_{KYR}}{M_K} \left[ \bar{R}^\nu \Theta_{\nu\mu}(Z) Y \partial^\mu K + \bar{Y} (\partial^\mu K^\dagger) \Theta_{\mu\nu}(Z) R^\nu \right], \quad (2.10)$$

$$\mathcal{L}_{\gamma p R}^{(1)} = \frac{ie g_1}{2M_p} \left[ \bar{R}^\nu \Theta_{\mu\lambda}(Y) \gamma_\nu \gamma^5 N F^{\nu\lambda} + \bar{N} \gamma^5 \gamma_\nu \Theta_{\lambda\mu}(Y) R^\mu F^{\nu\lambda} \right], \quad (2.11)$$

$$\mathcal{L}_{\gamma p R}^{(2)} = \frac{-e g_2}{4M_p^2} \left[ \bar{R}^\mu \Theta_{\mu\nu}(X) \gamma^5 (\partial_\lambda N) F^{\nu\lambda} - (\partial_\lambda \bar{N}) \gamma^5 \Theta_{\nu\mu}(X) R^\mu F^{\nu\lambda} \right]. \quad (2.12)$$

In expression (2.10),  $\mathcal{L}_{KYR}$  specifies the Lagrangian for the strong Kaon-Hyperon-Resonance ( $KYR$ ) vertex in which  $K$  denotes the iso-doublet

$$K = \begin{pmatrix} K^+ \\ K^0 \end{pmatrix}.$$

$\mathcal{L}^{(1)}$  and  $\mathcal{L}^{(2)}$  are for the  $\gamma^5$  and *derivative* electromagnetic coupling terms, respectively. There  $F^{\mu\nu}$  is the standard electromagnetic field tensor, and  $\Theta_{\mu\nu}$  is defined as (for our choice of  $A = -1$  in the previous Subsection)

$$\Theta_{\mu\nu}(V) = g_{\mu\nu} - (V + \frac{1}{2})\gamma_\mu\gamma_\nu. \quad (2.13)$$

It is important to stress that in the above Lagrangian,  $V = X, Y, Z$  are arbitrary parameters which conserve the symmetry of the free Lagrangian under the point transformation [Eq. (2.3)], and are often called the *off-shell parameters*. As will become clear later, we shall exploit this extra freedom to make the kaon electromagnetic production amplitudes well tamed. In what follows we shall rather use  $\tilde{X} \equiv X + \frac{1}{2}$ ,  $\tilde{Y} \equiv 2Y + 1$ ,  $\tilde{Z} \equiv Z + \frac{1}{2}$ .

The contribution to the  $S$ -matrix from the  $s$ -channel resonance pole through the  $\gamma^5$  coupling reads

$$S_2^{(s)} = \frac{i^2}{2!} \int d^4x_2 d^4x_1 T\{\mathcal{L}_{KYR}(x_2)\mathcal{L}_{\gamma pR}^{(1)}(x_1)\}, \quad (2.14)$$

where  $T$  is the time-ordering operator. Using the above Lagrangians, the matrix element for the  $\gamma^5$  term is obtained as

$$\begin{aligned} \langle YK|T_s^{(1)}|\gamma p\rangle &= -iG_1\bar{U}_Y(\mathbf{p}_Y)ip_K^\eta\Theta_{\eta\mu}(Z)P^{\mu\nu}(q) \\ &\quad \times \Theta_{\nu\chi}(Y)\gamma_\beta\gamma^5[-ip_\gamma^\beta\epsilon^\chi + i\epsilon^\beta p_\gamma^\chi]U_p(\mathbf{p}_p), \end{aligned} \quad (2.15)$$

where we have introduced the coupling constant

$$G_1 \equiv \frac{eg_1g_{KYR}}{2M_pM_K}, \quad (2.16)$$

$\epsilon^\chi$  is the polarization vector of the photon,  $q = p_\gamma + p_p = p_K + p_Y$  is the total momentum ( $s = q^2$ ), and  $P^{\mu\nu}(q)$  is the spin-3/2 propagator introduced in the last Subsection, Eq.(2.9).

Using expression (2.13) for  $\Theta_{\mu\nu}$  to calculate the terms on both sides of the propagator, we find

$$\begin{aligned} \langle YK|T_s^{(1)}|\gamma p\rangle &= -iG_1\bar{U}_Y(\mathbf{p}_Y)[(p_K)_\mu - \tilde{Z}\not{p}_K\gamma_\mu]P^{\mu\nu}(q) \\ &\quad \times \left\{ [\epsilon_\nu\not{p}_\gamma - (p_\gamma)_\nu\not{\epsilon}] - \tilde{Y}\gamma_\nu[\not{\epsilon}\not{p}_\gamma - \epsilon\cdot p_\gamma] \right\} \gamma^5 U_p(\mathbf{p}_p). \end{aligned} \quad (2.17)$$

A similar calculation leads to the *derivative* coupling contribution corresponding to  $\mathcal{L}^{(2)}$

$$\begin{aligned} \langle YK|T_s^{(2)}|\gamma p\rangle &= -iG_2\bar{U}_Y(\mathbf{p}_Y)[(p_K)_\mu - \tilde{Z}\not{p}_K\gamma_\mu]P^{\mu\nu}(q) \\ &\quad \times \left\{ [\epsilon\cdot p_p(p_\gamma)_\nu - p_\gamma\cdot p_p\epsilon_\nu] + \tilde{X}\gamma_\nu[p_\gamma\cdot p_p\not{\epsilon} - \epsilon\cdot p_p\not{p}_\gamma] \right\} \gamma^5 U_p(\mathbf{p}_p), \end{aligned} \quad (2.18)$$

with

$$G_2 \equiv \frac{eg_2g_{KYR}}{4M_p^2M_K}. \quad (2.19)$$

### C. Vertex functions

Adding the above two contributions given in Eqs. (2.17) and (2.18), we can write the scattering amplitude  $M_{fi}$  corresponding to the  $s$ -channel exchange of an  $S^P = 3/2^+$  resonance as

$$M_{fi}^{(s)} = \bar{U}_Y(\mathbf{p}_Y) \mathcal{V}^\mu(KYR) P_{\mu\nu}(q) \mathcal{V}^\nu(Rp\gamma) U_p(\mathbf{p}_p), \quad (2.20)$$

where the  $(KYR)$  vertex reads

$$\mathcal{V}^\mu(KYR) = -\frac{g_{KYR}}{M_K} [p_K^\mu - \tilde{Z} \not{p}_K \gamma^\mu], \quad (2.21)$$

and the  $(Rp\gamma)$  vertex is

$$\begin{aligned} \mathcal{V}^\nu(Rp\gamma) = & \left[ \frac{eg_1}{2M_p} (\epsilon^\nu \not{p}_\gamma - p_\gamma^\nu \not{\epsilon} - \tilde{Y} \gamma^\nu (\not{\epsilon} \not{p}_\gamma - \epsilon \cdot p_\gamma)) \right. \\ & \left. + \frac{eg_2}{4M_p^2} (\epsilon \cdot p_p \not{p}_\gamma^\nu - p_\gamma \cdot p_p \epsilon^\nu + \tilde{X} \gamma^\nu (p_\gamma \cdot p_p \not{\epsilon} - \epsilon \cdot p_p \not{p}_\gamma)) \right] i\gamma^5. \end{aligned} \quad (2.22)$$

Note that, for the general case of electroproduction, the above vertex must be multiplied by  $F^R = F_2^p$ , the second Dirac form factor of the proton. In the case of photoproduction, this factor reduces to unity, and in addition we have  $\epsilon \cdot p_\gamma = 0$ .

### D. Invariant amplitudes

The Lorentz invariant matrix element for electroproduction is written as

$$M_{fi}^{(s)} = i \bar{U}_Y \left( \sum_{j=1}^6 \mathcal{A}_j \mathcal{M}_j \right) U_p, \quad (2.23)$$

where  $\bar{U}_Y$  and  $U_p$  are the spinors of the hyperon and the proton, respectively,  $\mathcal{A}_j$ 's are Lorentz invariant scalar functions of the Mandelstam variables, and  $\mathcal{M}_j$ 's are the six usual gauge invariant matrices for the electroproduction

$$\begin{aligned} \mathcal{M}_1 &= \gamma^5 (\not{p}_\gamma \not{\epsilon} - \epsilon \cdot p_\gamma), \\ \mathcal{M}_2 &= 2\gamma^5 (\epsilon \cdot p_p p_\gamma \cdot p_Y - \epsilon \cdot p_Y p_\gamma \cdot p_p), \\ \mathcal{M}_3 &= \gamma^5 (\not{\epsilon} p_\gamma \cdot p_p - \not{p}_\gamma \epsilon \cdot p_p), \\ \mathcal{M}_4 &= \gamma^5 (\not{\epsilon} p_\gamma \cdot p_Y - \not{p}_\gamma \epsilon \cdot p_Y), \\ \mathcal{M}_5 &= \gamma^5 (p_\gamma^2 \not{\epsilon} - \epsilon \cdot p_\gamma \not{p}_\gamma), \end{aligned}$$

$$\mathcal{M}_6 = \gamma^5 (p_\gamma^2 \epsilon \cdot p_Y - \epsilon \cdot p_\gamma p_\gamma \cdot p_Y) - \gamma^5 (p_\gamma^2 \epsilon \cdot p_p - \epsilon \cdot p_\gamma p_\gamma \cdot p_p). \quad (2.24)$$

Due to the second term,  $-\gamma^5 (p_\gamma^2 \epsilon \cdot p_p - \epsilon \cdot p_\gamma p_\gamma \cdot p_p)$ , the choice of  $\mathcal{M}_6$  is different from that used in Refs. [3] and [1]. This results in a few modifications in the expressions of the CGLN amplitudes for the electroproduction as given in Appendix A. The advantage of this choice is its symmetric property under the exchange  $p_p \leftrightarrow -p_Y$ , thus leading to more transparent relations between the  $s$ - and  $u$ -channels amplitudes, as shown in the next section. In the case of photoproduction, ( $p_\gamma^2 = 0$ ,  $\epsilon \cdot p_\gamma = 0$ ), only the first four invariant amplitudes in Eq. (2.24) are needed.

Using the above expressions for the propagator and vertices, application of the Dirac algebra leads to the invariant amplitudes  $\mathcal{A}_j$ , which are expressed as sums of resonant or pole ( $P$ ) and non-pole ( $NP$ ) contributions. In the case of the photoproduction we find

$$\mathcal{A}_j = \sum_{i=1}^2 G_i \left[ \frac{P_{ij}^P}{s - M_R^2} + P_{ij}^{NP} \right] \quad , \quad (j = 1, \dots, 4), \quad (2.25)$$

The expressions of the  $P_{ij}^{P,NP}$  coefficients are given in Appendix B, Eqs. (B9) to (B11).

The electroproduction amplitudes can be written in a similar form

$$\mathcal{A}_j = \sum_{i=1}^2 G_i \left[ \frac{E_{ij}^P}{s - M_R^2} + E_{ij}^{NP} \right] \quad , \quad (j = 1, \dots, 6). \quad (2.26)$$

For  $j = 1, \dots, 4$ , the  $E_{ij}^{P,NP}$  coefficients are expressed in terms of the above defined photoproduction coefficients  $P_{ij}^{P,NP}$  as

$$E_{ij}^{P,NP} = P_{ij}^{P,NP} + p_\gamma^2 R_{ij}^{P,NP} \quad , \quad (i = 1, 2) \quad , \quad (j = 1, \dots, 4). \quad (2.27)$$

The extra terms  $R_{ij}^{P,NP}$  are given in Appendix B, Eqs. (B13) and (B14). Note that this decomposition is not necessary for  $j = 5, 6$ . The corresponding coefficients  $E_{ij}^{P,NP}$  are given in Eqs. (B15) and (B16) of Appendix B.

Note that in the calculation of the observables (Sec. IV), the following replacement is made in the denominator of the pole contribution in Eqs. (2.25) and (2.26)

$$s - M_R^2 \rightarrow s - M_R^2 + iM_R\Gamma_R, \quad (2.28)$$

where  $\Gamma_R$  is the width of the resonance.

It should be important to emphasize here that the *pole* contributions (see Appendix B) are completely *independent* of  $V(= X, Y, Z)$ , hence with no off-shell dependence.



So far we have discussed the case in which the parity of the  $s$ -channel resonance is positive. For a resonance with negative parity, we have only to make the following replacements:  $\mathcal{V}^\mu(KYR) \rightarrow i\gamma^5\mathcal{V}^\mu(KYR)$  in Eq. (2.21), and  $i\gamma^5 \rightarrow 1$  in Eq. (2.22). In the corresponding  $M_{fi}$  amplitude [Eq. (2.20)],  $\gamma^5$  is now acting onto the left of the first vertex. Using the anti-commutation property of  $\gamma^5$  with  $\gamma^\mu$ , it is easy to move the  $\gamma^5$  matrix in the same position as in the positive parity case, namely onto the right of the second vertex. By inspection, we immediately obtain the parity rule for the invariant (pole and non-pole) amplitudes

$$E_{ij}^{(-)}(M_R) = (-)^{i+1}E_{ij}^{(+)}(-M_R) \quad , \quad (i = 1, 2) \quad , \quad (j = 1, \dots, 6). \quad (2.29)$$

## E. Formalisms without off-shell effects

### 1. Renard and Renard approach

The expressions used in Ref. [2] for the propagator is the same as Eq. (2.9), but in the interaction Lagrangian Eqs. (2.10)-(2.12)  $\Theta_{\mu\lambda}(V)$ , ( $V = X, Y, Z$ ) was set equal to  $g_{\mu\lambda}$ . In other words, the authors put  $V \equiv -\frac{1}{2}$  in (2.13) (or  $\tilde{V} \equiv 0$ ), thus no off-shell effect associated with the spin 3/2 particles was considered. It is therefore clear from Eqs. (2.21) and (2.22) that the corresponding amplitude simplifies considerably. However, some of the *non-pole* contributions  $P_{ij}^{NP}$  grow linearly in the  $s$ -variable (see Appendix B), causing an undesirable increase, for example, in the production cross section. For this reason *all* the resulting *non-pole* contributions were artificially thrown away in Ref. [2].

### 2. Adelseck et al. approach

To avoid the difficulties encountered in the Renard & Renard model [2], Adelseck *et al.* [3] have suggested and applied the following prescriptions (used also in Ref. [1]). The propagator is written from Eq. (2.9), with the mass of the resonance  $M_R$  replaced by the total invariant energy  $\sqrt{s}$ , except in the denominator where the width of the resonance is introduced

$$P_{\mu\nu}^A = \frac{\not{q} + \sqrt{s}}{3(s - M_R^2 + iM_R\Gamma_R)} \left[ 3g_{\mu\nu} - \gamma_\mu\gamma_\nu - \frac{2}{s}q_\mu q_\nu - \frac{1}{\sqrt{s}}(\gamma_\mu q_\nu - \gamma_\nu q_\mu) \right]. \quad (2.30)$$

This modification provides an extra damping of the amplitude with increasing channel energy. So together with the corresponding modification in the vertices discussed below, an

unwanted growth in the production cross section due to the non-pole contribution could be reduced in the absence of the off-shell freedom (in terms of  $X, Y, Z$ ).

In the photoproduction case, the  $KYR$  vertex is

$$\mathcal{V}^\mu(KYR) = \frac{\tilde{g}_{KYR}}{M_R} p_Y^\mu, \quad (2.31)$$

and the  $Rp\gamma$  vertex factor for a positive parity resonance is written as

$$\mathcal{V}^\nu(Rp\gamma) = i \left[ g_a \left( \epsilon^\nu - \frac{p_\gamma^\nu \not{\epsilon}}{\sqrt{s} + M_p} \right) + g_b \frac{1}{(\sqrt{s} + M_p)^2} (\epsilon \cdot p_p p_\gamma^\nu - p_\gamma \cdot p_p \epsilon^\nu) \right] \gamma^5. \quad (2.32)$$

As stated by Adelseck *et al.*, these prescriptions were used to ensure gauge invariance of the scattering amplitude. In fact, expressions (2.31) and (2.32) may be reached from Eqs. (2.21) and (2.22) as demonstrated in Appendix C, where the coupling constants  $g_a$ ,  $g_b$ , and  $\tilde{g}_{KYR}$  are defined in terms of  $g_1$ ,  $g_2$ , and  $g_{KYR}$ , respectively. Particularly, the photon coupling vertex in this choice contains damping factors in the  $s$ -variable.

However, regarding the spin 3/2 propagator (2.30), when the same form is used for a  $u$ -channel resonance exchange, namely the  $s$ -variable replaced by the  $u$ -variable, the latter may vanish at certain kinematical situations, leading to an unphysical behavior. Note also that as pointed out in [5], such propagators do not have inverses, and corresponding wave equations for the the spin-3/2 field can not be defined. Thus this approach is not appropriate for a consistent simultaneous description of the  $s$ - and  $u$ -channels.

### III. SPIN 3/2 RESONANCES IN THE $U$ -CHANNEL

#### A. Direct calculation

In this section we show some basic details on how the lowest order  $u$ -channel exchange of a  $\Lambda^*(3/2^+)$  resonance contributes to the amplitude for  $K^+$  production on the proton. The exchange of a  $\Lambda^*(3/2^+)$  resonance in the  $u$ -channel is treated along the same lines as in section II for the  $s$ -channel resonances exchange. The part of the  $S$ -matrix corresponding to the  $\gamma^5$  photon coupling is

$$S_2^{(u)} = \frac{i^2}{2!} \int d^4x_2 d^4x_1 T\{\mathcal{L}_{\gamma YR}^{(1)}(x_2)\mathcal{L}_{KpR}(x_1)\}, \quad (3.1)$$

with  $R \equiv \Lambda^*(3/2^+)$ . The resulting matrix element takes the form

$$\begin{aligned} \langle YK|T_u^{(1)}|\gamma p \rangle = & \frac{-ieg'_1 g_{KpR}}{2M_Y M_K} \bar{U}_Y(\mathbf{p}_Y) \gamma_5 \gamma_\beta [-ip_\gamma^\beta \epsilon^\lambda + i\epsilon^\beta p_\gamma^\lambda] \Theta_{\lambda\nu}(Y) \\ & \times P^{\nu\mu}(-q') \Theta_{\mu\chi}(Z) i p_K^\chi U_p(\mathbf{p}_p). \end{aligned} \quad (3.2)$$

The momentum transfer is  $q' \equiv p_\gamma - p_Y = p_K - p_p$ , with  $q'^2 = u$ . Note that with a correct kinematical consideration it is easy to see that the propagator depends on  $-q'$  (not  $q'$ !).

Using Eq. (2.13) just as before, one finds

$$\begin{aligned} \langle YK|T_u^{(1)}|\gamma p \rangle = & \frac{-ieg'_1 g_{KpR}}{2M_Y M_K} \bar{U}_Y(\mathbf{p}_Y) \gamma_5 \{ [\epsilon_\nu \not{p}_\gamma - (p_\gamma)_\nu \not{\epsilon}] - \tilde{Y} [\not{p}_\gamma \not{\epsilon} - \epsilon \cdot p_\gamma] \gamma_\nu \} \\ & \times P^{\nu\mu}(-q') [(p_K)_\mu - \tilde{Z} \gamma_\mu \not{p}_K] U_p(\mathbf{p}_p). \end{aligned} \quad (3.3)$$

The *derivative* coupling term is calculated along the same lines, leading to

$$\begin{aligned} \langle YK|T_u^{(2)}|\gamma p \rangle = & \frac{-ieg'_2 g_{KpR}}{4M_Y^2 M_K} \bar{U}_Y(\mathbf{p}_Y) \gamma_5 \{ [\epsilon \cdot p_Y (p_\gamma)_\nu - p_\gamma \cdot p_Y \epsilon_\nu] + \tilde{X} [p_\gamma \cdot p_Y \not{\epsilon} - \epsilon \cdot p_Y \not{p}_\gamma] \gamma_\nu \} \\ & \times P^{\nu\mu}(-q') [(p_K)_\mu - \tilde{Z} \gamma_\mu \not{p}_K] U_p(\mathbf{p}_p). \end{aligned} \quad (3.4)$$

In the above expressions,  $g'_1$  and  $g'_2$  are the two  $\gamma YR$  coupling constants, which are similar to  $g_1$  and  $g_2$  as in Eqs. (2.11) and (2.12). Note the similarity of the last two expressions with the corresponding ones for an  $s$ -channel resonance exchange, Eqs. (2.17) and (2.18). Adding the two above contributions, the scattering matrix in the  $u$ -channel exchange reads

$$M_{fi}^{(u)} = \bar{U}_Y(\mathbf{p}_Y) \mathcal{V}^\nu(RY\gamma) P_{\nu\mu}(-q') \mathcal{V}^\mu(KpR) U_p(\mathbf{p}_p). \quad (3.5)$$

The two vertices are

$$\mathcal{V}^\mu(KpR) = -\frac{g_{KpR}}{M_K} [p_K^\mu - \tilde{Z}\gamma^\mu \not{p}_K], \quad (3.6)$$

$$\begin{aligned} \mathcal{V}^\nu(RY\gamma) = i\gamma_5 \left[ \frac{eg'_1}{2M_Y} (\epsilon^\nu \not{p}_\gamma - p_\gamma^\nu \not{\epsilon} - \tilde{Y}(\not{p}_\gamma \not{\epsilon} - \epsilon \cdot p_\gamma) \gamma^\nu) \right. \\ \left. + \frac{eg'_2}{4M_Y^2} (\epsilon \cdot p_Y p_\gamma^\nu - p_\gamma \cdot p_Y \epsilon^\nu + \tilde{X}(p_\gamma \cdot p_Y \not{\epsilon} - \epsilon \cdot p_Y \not{p}_\gamma) \gamma^\nu) \right]. \end{aligned} \quad (3.7)$$

The propagator reads

$$P_{\nu\mu}(-q') = \frac{-\not{q}' + M_R}{3(u - M_R^2)} \left[ 3g_{\nu\mu} - \gamma_\nu \gamma_\mu - \frac{2}{M_R^2} q'_\nu q'_\mu + \frac{1}{M_R} (\gamma_\nu q'_\mu - \gamma_\mu q'_\nu) \right]. \quad (3.8)$$

Using the above expressions for the vertices and propagator, the decomposition of  $M_{fi}^{(u)}$  in terms of the gauge invariant matrices defined in Eq. (2.24) can be done along the same lines as in section II.D. However, comparing the  $s$ - and  $u$ -channels vertices and propagators, it is easy to get out the rules regarding how to obtain the expressions for the  $u$ -channel exchange from those for the  $s$ -channel, namely: 1) exchange  $p_p \leftrightarrow -p_Y$  (including  $M_N \rightarrow M_Y$ ), 2) express the products of  $\gamma$  matrices in a reversed order, 3) change  $s \rightarrow u$ ,  $g_2 \rightarrow -g_2$ ,  $M_R \rightarrow -M_R$ , and 4) exchange the two vertices and put the appropriate coupling constants. In fact, these rules result from a substitution rule which is simpler to use, since it allows us to formally derive the invariant amplitudes for the  $u$ -channel exchange directly from the corresponding  $s$ -channel exchange amplitudes. The derivation of the substitution rule and its application to obtain the invariant amplitudes are given in the next two Subsections.

## B. Substitution rule

We now calculate the  $u$ -channel results by substitution rule applied to the  $s$ -channel expressions. Namely, we introduce in Eq. (2.20) the appropriate coupling constants, together with the following replacements:  $s \rightarrow u$ ,  $M_N \rightarrow M_Y$ ,  $p_p \leftrightarrow -p_Y$ ,  $U_p(\mathbf{p}_p) \rightarrow V_Y(-\mathbf{p}_Y)$ ,  $U_Y(\mathbf{p}_Y) \rightarrow V_p(-\mathbf{p}_p)$ , with  $V_p, V_Y$  being the negative energy spinors. The resulting scattering matrix is

$$M_{fi}^{(u)} = \overline{V}_p(-\mathbf{p}_p) \mathcal{V}^\mu(KpR) P_{\mu\nu}(q') \mathcal{V}^\nu(RY\gamma) V_Y(-\mathbf{p}_Y), \quad (3.9)$$

and the expressions of the vertices and propagator are [cf. Eqs. (2.21), (2.22), and (2.9)]:

$$\mathcal{V}^\mu(K^R) = -\frac{g_{KpR}}{M_K} [p_K^\mu - \tilde{Z}\not{p}_K\gamma^\mu], \quad (3.10)$$

$$\begin{aligned} \mathcal{V}^\nu(RY\gamma) = i \left[ \frac{eg'_1}{2M_Y} (\epsilon^\nu \not{p}'_\gamma - p'_\gamma{}^\nu \not{\epsilon} - \tilde{Y} \gamma^\nu (\not{\epsilon} \not{p}'_\gamma - \epsilon \cdot p_\gamma)) \right. \\ \left. - \frac{eg'_2}{4M_Y^2} (\epsilon \cdot p_Y p'_\gamma{}^\nu - p_\gamma \cdot p_Y \epsilon^\nu + \tilde{X} \gamma^\nu (p_\gamma \cdot p_Y \not{\epsilon} - \epsilon \cdot p_Y \not{p}'_\gamma)) \right] \gamma_5, \end{aligned} \quad (3.11)$$

$$P_{\mu\nu}(q') = \frac{q' + M_R}{3(u - M_R^2)} \left[ 3g_{\mu\nu} - \gamma_\mu \gamma_\nu - \frac{2}{M_R^2} q'_\mu q'_\nu - \frac{1}{M_R} (\gamma_\mu q'_\nu - \gamma_\nu q'_\mu) \right], \quad (3.12)$$

with  $q' = p_\gamma - p_Y = p_K - p_p$ , as before.

Using the relation between the  $V$  and  $U$  spinors:  $V(-\mathbf{p}) = C \bar{U}^T(\mathbf{p})$ , with  $C = \gamma_0 \gamma_2$  the charge conjugation operator, and  $\bar{U} = U^\dagger \gamma_0$  the Dirac adjoint of  $U$ , Eq. (3.9) is written as:

$$M_{fi}^{(u)} = -U_p^T(\mathbf{p}_p) C^{-1} \mathcal{V}^\mu(KpR) P_{\mu\nu}(q') \mathcal{V}^\nu(RY\gamma) C \bar{U}_Y^T(\mathbf{p}_Y), \quad (3.13)$$

By appropriately inserting  $I = C^{-1}C$ , the above equation can be transformed into

$$M_{fi}^{(u)} = -\bar{U}_Y(\mathbf{p}_Y) [\mathcal{V}^\nu(RY\gamma)^T]^C [P_{\mu\nu}(q')^T]^C [\mathcal{V}^\mu(KpR)^T]^C U_p(\mathbf{p}_p), \quad (3.14)$$

where we have defined the  $C$ -transform of  $X^T$  as

$$[X^T]^C = C^{-1} X^T C.$$

Now, we exploit the properties of the charge conjugation matrix  $C$  to calculate the  $C$ -transforms of the vertices and propagator. For example, the  $C$ -transform of the  $(KpR)$  vertex Eq.(3.10) is

$$[\mathcal{V}^\mu(KpR)^T]^C = -\frac{g_{KpR}}{M_K} C^{-1} [p_K^\mu - \tilde{Z} \not{p}'_K \gamma^\mu]^T C. \quad (3.15)$$

From the properties of  $C$ , we obtain

$$C^{-1} (\not{p}'_K \gamma^\mu)^T C = C^{-1} \gamma^{\mu T} (p_K)_\nu \gamma^{\nu T} C = \gamma^\mu (p_K)_\nu \gamma^\nu = \gamma^\mu \not{p}'_K, \quad (3.16)$$

and Eq. (3.15) becomes

$$[\mathcal{V}^\mu(KpR)^T]^C = -\frac{g_{KpR}}{M_K} [p_K^\mu - \tilde{Z} \gamma^\mu \not{p}'_K], \quad (3.17)$$

A similar calculation leads to the  $RY\gamma$  vertex

$$\begin{aligned} [\mathcal{V}^\nu(RY\gamma)^T]^C = i\gamma_5 \left[ -\frac{eg'_1}{2M_Y} (\epsilon^\nu \not{p}'_\gamma - p'_\gamma{}^\nu \not{\epsilon} - \tilde{Y} (\not{p}'_\gamma \not{\epsilon} - \epsilon \cdot p_\gamma) \gamma^\nu) \right. \\ \left. - \frac{eg'_2}{4M_Y^2} (\epsilon \cdot p_Y p'_\gamma{}^\nu - p_\gamma \cdot p_Y \epsilon^\nu + \tilde{X} (p_\gamma \cdot p_Y \not{\epsilon} - \epsilon \cdot p_Y \not{p}'_\gamma) \gamma^\nu) \right], \end{aligned} \quad (3.18)$$

and the propagator takes the form

$$[P_{\mu\nu}(q')^T]^C = \frac{-\not{q}' + M_R}{3(u - M_R^2)} \left[ 3g_{\nu\mu} - \gamma_\nu\gamma_\mu - \frac{2}{M_R^2} q'_\nu q'_\mu + \frac{1}{M_R} (\gamma_\nu q'_\mu - \gamma_\mu q'_\nu) \right]. \quad (3.19)$$

Comparing with Eq. (3.12) leads to

$$[P_{\mu\nu}(q')^T]^C = P_{\nu\mu}(-q'). \quad (3.20)$$

Combining Eqs. (3.14), (3.17), (3.18) and (3.20) leads to the same result as the direct calculation Eqs. (3.5)-(3.8).

### C. Invariant amplitudes

In this subsection, we apply the substitution rule to obtain the invariant amplitudes (hereafter denoted as  $\mathcal{A}'_j$ ) for the  $u$ -channel exchange directly from the corresponding  $s$ -channel exchange amplitudes  $\mathcal{A}_j$ .

Let us write Eq. (2.23) with specifying the relevant variables

$$M_{fi}^{(s)} = i \bar{U}_Y(\mathbf{p}_Y) \left( \sum_{j=1}^6 \mathcal{A}_j(s, t, u) \mathcal{M}_j(p_p, p_Y) \right) U_p(\mathbf{p}_p). \quad (3.21)$$

where  $\mathcal{M}_j$  are the six gauge invariant amplitudes Eq.(2.24), and  $\mathcal{A}_j$  have been made explicit in section II.D. We now apply the substitution rule (see the previous subsection) to Eq. (3.21) in order to obtain the scattering matrix in the  $u$ -channel

$$M_{fi}^{(u)} = i \bar{V}_p(-\mathbf{p}_p) \left( \sum_{j=1}^6 \mathcal{A}_j(u, t, s) \mathcal{M}_j(-p_Y, -p_p) \right) V_Y(-\mathbf{p}_Y). \quad (3.22)$$

From Eq. (2.24), it is clear that

$$\begin{aligned} \mathcal{M}_{1,5,6}(-p_Y, -p_p) &= \mathcal{M}_{1,5,6}(p_p, p_Y), \\ \mathcal{M}_2(-p_Y, -p_p) &= -\mathcal{M}_2(p_p, p_Y), \quad \mathcal{M}_{3,4}(-p_Y, -p_p) = -\mathcal{M}_{4,3}(p_p, p_Y). \end{aligned} \quad (3.23)$$

We proceed as in the last subsection, and transform Eq. (3.22) into

$$M_{fi}^{(u)} = -i \bar{U}_Y(\mathbf{p}_Y) \left( \sum_{j=1}^6 \mathcal{A}_j(u, t, s) C^{-1} \mathcal{M}_j^T(-p_Y, -p_p) C \right) U_p(\mathbf{p}_p), \quad (3.24)$$

Then, we calculate the  $C$ -transforms of the  $\mathcal{M}_j^T(-p_Y, -p_p)$  matrices, which can easily be expressed in terms of the original  $\mathcal{M}_j(p_p, p_Y)$  matrices as

$$\begin{aligned}
C^{-1} \mathcal{M}_{1,2}^T(-p_Y, -p_p) C &= -\mathcal{M}_{1,2}(p_p, p_Y), \\
C^{-1} \mathcal{M}_{5,6}^T(-p_Y, -p_p) C &= \mathcal{M}_{5,6}(p_p, p_Y), \\
C^{-1} \mathcal{M}_{3,4}^T(-p_Y, -p_p) C &= \mathcal{M}_{4,3}(p_p, p_Y).
\end{aligned} \tag{3.25}$$

Substituting these relations into Eq. (3.24), the scattering matrix in the  $u$ -channel can be written as

$$M_{fi}^{(u)} = i \bar{U}_Y(\mathbf{p}_Y) \left( \sum_{j=1}^6 \mathcal{A}'_j(s, t, u) \mathcal{M}_j(p_p, p_Y) \right) U_p(\mathbf{p}_p), \tag{3.26}$$

where the invariant amplitudes  $\mathcal{A}'_j$  are related to the  $\mathcal{A}_j$  amplitudes in the  $s$ -channel as follows

$$\mathcal{A}'_{1,2}(s, t, u) = \mathcal{A}_{1,2}(u, t, s), \quad \mathcal{A}'_{3,4}(s, t, u) = \mathcal{A}_{4,3}(u, t, s), \quad \mathcal{A}'_{5,6}(s, t, u) = -\mathcal{A}_{5,6}(u, t, s). \tag{3.27}$$

It is then quite easy to obtain these invariant amplitudes in a form similar to Eq. (2.26), which we will not present in this article.

## IV. RESULTS AND DISCUSSION

In this section we *illustrate* the sensitivity of different  $K\Lambda$  channels observables to the off-shell effects. We need, hence, a reliable dynamical model, with respect to the existing data, as starting point. In the following, we present first how a rather simple model was obtained and then, within the dynamical ingredients required by the available data, we report on the importance of the off-shell effects according to the observables and/or the phase space regions investigated.

### A. Reaction mechanism

To build a simple model with a reasonably realistic dynamical content, we take advantage of the SL model [1] which has emerged from a comprehensive phenomenological study.

The underlying dynamics in the SL model is, besides extended Born terms, resonances exchanges (Table I) in the following channels:

- *s-channel*:  $N1(1/2)$ ,  $N7(3/2)$ ,  $N8(5/2)$  ; where the spin of each nucleonic resonance is given in parenthesis.
- *u-channel*:  $L1$ ,  $L3$ ,  $L5$ ,  $S1$  ; all spin  $1/2$  hyperonic resonances.
- *t-channel*:  $K^*$ ,  $K1$  ; both of them have also been included in the present work and we will not discuss them any further.

In the *s*-channel, the most relevant resonance, in the frame of the present work, is the spin  $3/2$  resonance  $N7$ . The  $N1$  resonance,  $P_{11}(1440)$ , was found to have a coupling compatible with zero (see Table I and Ref. [1]). Moreover, a recent model-independent nodal structure analysis [10] concludes that the present data do not require contributions from the  $P_{11}$  resonances. Concerning another nucleonic resonance in the SL model, the  $N8(5/2)$ , it was shown [1] that its contribution to the considered underlying dynamics *is not crucial* (see Table XI in Ref. [1]).

For these reasons, *we removed the  $N1$  and  $N8$  resonances in searching for a simple model to study the role of off-shell effects*. The parameters of this model, hereafter called model A, have been obtained by re-fitting the data. Note that the formalism used in this re-fitting is still within the context of Adelseck *et al.*'s treatment for the spin  $3/2$  resonance  $N7$ . Model A is the basis of our numerical results reported in the next subsection.



The first step was thus, using model A, to fit the same data base as used to obtain the SL model (all available 312 data points for photo-, electro-production, as well as for the  $K^-p$  radiative capture process). The coupling constants and the reduced  $\chi^2$  are given in Table I. Although the resultant  $\chi^2$  for model A (1.84) is slightly larger than that for the SL model (1.73), it is still acceptable. Anticipating the presentation of the observables in the next subsection, the fit of the data with model A appears at a comparable level of quality as with the SL model, see the dotted and dash-dotted curves in Figs. 1-3, and Fig. 5. Hence, these results justify the use of model A as a starting point to investigate the sensitivity of the observables to the off-shell effects.

Given that model A contains only one spin 3/2 baryonic resonance, we have also investigated possible contributions from other known spin 3/2 nucleonic resonances, namely<sup>3</sup>,  $[N(1520)[(2)\frac{3}{2}^-]$  ( $N2$ ) or  $[N(1700)[(2)\frac{3}{2}^-]$  ( $N5$ ). We performed minimizations for all possible configurations including one to three of the spin 3/2 resonances  $N2$ ,  $N5$ , and  $N7$ . In these configurations, whenever at least one of the two resonances  $N2$ , and  $N5$  was retained, the corresponding  $\chi^2$ 's were found significantly larger than that for model A, implying that the existing data base does not require contributions from these resonances. Through the numerical investigations mentioned above, we have re-confirmed that model A is indeed a *reasonable starting model* for the present study.

Then we adopted the correct propagator [Eq. (2.9)] and introduced the off-shell treatments to the  $N7$  resonance, and fitted again the data to obtained model B (Table I). Finally, for the sake of completeness we included the  $u$ -channel spin 3/2 hyperonic resonance  $[\Lambda(1890)[(0)\frac{3}{2}^+]$  ( $L8$ ) with the off-shell effect, and once again fitted the data (model C in Table I). The choice of this resonance, as in the case of nucleonic resonances mentioned above, comes from the fact that the inclusion of any other spin 3/2 hyperonic resonance,  $[\Lambda(1520)[(0)\frac{3}{2}^-]$  ( $L6$ ) or  $[\Lambda(1690)[(0)\frac{3}{2}^-]$  ( $L7$ ), deteriorates the reduced  $\chi^2$  significantly.

Here we would like to point out that by adding any spin 3/2 baryonic resonance we introduce five additional free parameters, namely two coupling constants ( $G_1$  and  $G_2$ ) and three off-shell parameters. The fact that the  $\chi^2$  associated with model C comes out larger than that for the model B, indicates that the dynamical content of the phenomenological approach discussed here is reliable enough, since *additional free parameters* due to apparently

---

<sup>3</sup>We use the notation  $[(\ell)J^\pi]$ .

unrelevant resonances *do not improve* the  $\chi^2$  (reduced or per point).

Model D in Table I, with two of the free parameters fixed, will be discussed in Subsec. C.

## B. Observables

In this subsection, we compare with the data the results of the four dynamical models (SL, A, B, and C) summarized in Table I. Here we will adhere closely to the observables reported for the SL model [1], where a comprehensive discussion on other available phenomenological results [11,12] is also presented.

### 1. Reaction $\gamma + p \rightarrow K^+ + \Lambda$

In Fig. 1, angular distributions and excitation functions for the differential cross-section are shown. All the models reproduce the data almost equally well. However, the excitation functions at  $\theta_K^{cm} = 90^\circ$  [Fig. 1(b)] and  $150^\circ$  [Fig. 1(c)] split the four models into two families above  $E_\gamma^{lab} \approx 1.5$  GeV: in the backward hemisphere, both the SL and A models predict significantly larger cross sections than the two others (B and C) which embody the off-shell effects.

For the angular distributions [Fig. 1(d), 1(e), and 1(f)], the four models give similar results at  $E_\gamma^{lab} = 1.0$  and 1.45 GeV, while at the highest energy [ $E_\gamma^{lab} = 2.1$  GeV; Fig. 1(f)] the off-shell treatments produce drastic effects at backward angles.

A striking manifestation of the above behaviors can be seen while investigating the total cross section (Fig. 2). The long lasting shortcoming of the phenomenological models based on effective Lagrangian approaches is significantly cured by the inclusion of the off-shell effects<sup>4</sup>. Namely, the total cross-section does not any more show a diverging behavior above  $E_\gamma^{lab} \approx 1.5$  GeV (see also Fig. 5 in Ref. [1]).

In the explored phase space region, the excitation functions and angular distributions for single polarization asymmetries (Fig. 3) show significant sensitivity to the off-shell treatments above roughly 1.8 GeV for the  $\Lambda$ -polarization asymmetry ( $P$ ) and polarized target asymmetry ( $T$ ). In the case of the linearly polarized beam asymmetry ( $\Sigma$ ) the effects are

---

<sup>4</sup>Preliminary data from ELSA [18] for both differential cross section at about 2 GeV and the total cross section up to the same energy show trends similar to those of model B in Figures 1(f) and 2.

more drastic. Indeed, above  $E_\gamma^{lab} \approx 1.6$  GeV the off-shell treatments produce a sign change with sizeable magnitudes around 2 GeV.

The angular distributions for double polarization asymmetries, at  $E_\gamma^{lab} = 1.45$  and 2.1 GeV, are shown in Fig. 4. A general trend for these observables is that significant off-shell effects appear in the backward hemisphere. In the case of  $C_{x'}$  asymmetry, this sensitivity gets attenuated with increasing photon energy. For the other asymmetry ( $C_{z'}$ ) with circularly polarized beam, as well as for the two asymmetries ( $O_{x'}$  and  $O_{z'}$ ) with linearly polarized beam, the effects are, on the contrary, enhanced with increasing photon energy. It is worth noticing that the two models without off-shell treatments predict almost vanishing values for  $O_{x'}$  and  $O_{z'}$  asymmetries, while introducing these treatments results in a sign change and sizeable magnitudes for these asymmetries in the backward hemisphere.

We note that the curves depicted in Figures 1-4 split in two families depending on whether the off-shell effects are included (models B and C) or not (models SL and A).

## 2. Reaction $e + p \rightarrow e' + K^+ + \Lambda$

The cross section for the electroproduction process is given by

$$\frac{d\sigma}{d\Omega_K} = d\sigma_U + \epsilon_L d\sigma_L + \epsilon d\sigma_P \sin^2\theta \cos 2\phi + \sqrt{2\epsilon_L(1+\epsilon)} d\sigma_I \sin\theta \cos\phi, \quad (4.1)$$

with  $\theta$  the angle between the outgoing kaon and the virtual photon, and  $\phi$  the azimuthal angle between the kaon production plane and the electron scattering plane. Transverse and longitudinal polarization parameters  $\epsilon$  and  $\epsilon_L$ , respectively, are defined as

$$\epsilon = \left[ 1 - 2 \frac{|\mathbf{p}_\gamma|^2}{p_\gamma^2} \tan^2\left(\frac{\Psi}{2}\right) \right] \quad , \quad \epsilon_L = -\frac{p_\gamma^2}{p_{\gamma 0}^2} \epsilon, \quad (4.2)$$

with  $\Psi$  the angle between the momenta of the incoming and outgoing electrons. Moreover,  $d\sigma_U$  is the cross section for an unpolarized incident photon beam, and the term containing  $d\sigma_P$  is the asymmetry contribution of a transversally polarized beam. The cross section of a longitudinally polarized virtual photon is given by  $d\sigma_L$ , while  $d\sigma_I$  contains the interference effects between the longitudinal and transverse components of the beam.

In the figures shown in the remaining of this Section, the electromagnetic form factors used are the same as in the SL model (see Subsec. IV.D in Ref [1]).

Figure 5 shows the unpolarized component of the differential cross section  $d\sigma_{UL} = d\sigma_U + \epsilon_L d\sigma_L$ , [see Eq. (4.1)], as a function of the momentum transfer. All four models reproduce

the data equally well. We note again that models B and C give almost identical results. The predictions for different components of the cross section [Eq. (4.1)] are reported in Fig. 6. The transverse component (T) splits also the four curves in the same two families, with the off-shell effects producing significantly smaller values for this observable. On the contrary, these effects enhance the longitudinal (L) part. The transverse-longitudinal (TL) interference term shows similar sensitivities. Among the observables reported here, the (L) and (TL) terms are the only ones to produce the most sizeable differences between the models SL and A. Finally, the transverse-transverse (TT) interference term shows rather negligible dependence on the ingredient of the models.

Because of the above predictions on the suppression of the transverse component and the enhancement of the longitudinal one due to the off-shell treatments, the ratio  $R(t) = d\sigma_L/d\sigma_U$  is an interesting quantity to be investigated. This latter was already found appealing in the SL approach while examining the effects of hadrons electromagnetic form factors. Here, the off-shell treatments have sizeable effect (Fig. 7): the ratio  $R(t)$  between  $-t = 0.5$  and  $1.0 \text{ GeV}^2$  is increased by a factor of  $\approx 2$  to 4, due to such treatments.

### 3. Reaction $K^- + p \rightarrow \gamma + \Lambda$

The amplitudes of the strangeness photoproduction can be related by crossing symmetry [19] to those of  $K^-p$  radiative capture processes

$$K^- + p \rightarrow \gamma + \Lambda. \quad (4.3)$$

Here, the relevant quantity is the branching ratio defined as

$$BR = \frac{\Gamma(K^-p \rightarrow \gamma\Lambda)}{\Gamma(K^-p \rightarrow \text{all})}, \quad (4.4)$$

with stopped kaons.

In Table II, the results of the four models are compared with the only available data point. They all agree with the upper bound of the experimental result. Although in the SL model the presence of the  $N7$  resonance was found relevant in reproducing the measured branching ratio (see Table XI in Ref [1]), the off-shell treatments are not affecting this observable. This may be due to the fact that here we are dealing only with stopped kaons, and the reported behavior might be altered for kaons in flight.

Before ending this section, we wish to make a few comments on some general features of the findings summarized in Table I and/or depicted in Figures 1 to 7.

### C. Comments on free parameters

The models discussed in this paper embody 12 (model A) to 20 (model C) free parameters, see Table I. In this subsection, we emphasize that, in spite of rather large number of free parameters, our approach offers some meaningful insight into the dynamics of the strangeness electromagnetic production processes.

#### 1. Coupling constants

In the fitting procedures, the two main coupling constants (Table I),  $g_{K\Lambda N}$  and  $g_{K\Sigma N}$ , have been allowed to vary within their broken  $SU(3)$ -symmetry limits [11]. Given that for the other couplings we do not dispose of any reliable values or constraints, we will discuss their variations, within the corresponding uncertainties, according to the models ingredients and/or off-shell treatments. The values referred to concern models SL, A, B, and C in Table I.

- *s-channel*: no significant variations are observed.
- *u-channel*: In going from the SL model to model A, the couplings of the  $L5$  and  $S1$  resonances undergo variations of factor 2 to 3. Then the inclusion of off-shell effects (going from model A to B) brings them back close to their SL model values, stabilizing them for the C model. These two consecutive variations might come from the observation [1] that in the SL model these two resonances are rather strongly correlated. This fact, in the absence of any constraint, leads to large variations of the  $L5$  and  $S1$  coupling constants. However, the combined contribution of these resonances to the observables does not show any drastic variation.
- *t-channel*: Significant variations are noticed comparing SL model with the other ones. Notice that a spin  $5/2$  resonance present in the SL model has been removed in the other models. The global increase of the  $t$ -channel strengths when discarding a spin  $5/2$  resonance is a manifestation of the duality hypothesis (the interplay between  $s$ - and  $t$ -channel strengths) in the strangeness sector, as discussed in Ref. [21].

The above considerations indicate strongly that the underlying dynamics retained in this work are tightly constrained by the available data base. Hence, the reported sensitivities to

off-shell treatments are not likely to be altered significantly by the rest of the free parameters of the models introduced here.

## 2. Off-shell free parameters

In obtaining models B and C we have treated the three parameters ( $X$ ,  $Y$ , and  $Z$ ) as free ones. As shown in Table I, out of six off-shell parameters related to the N7 and L8 resonances, the largest one by far is the  $Y$  parameter for the N7 resonance. The  $Z$  parameter related to this latter resonance comes out to be compatible with zero. Moreover, all three parameters of the N7 resonance are stable upon comparing B and C models.

Notice that one of the main motivations in introducing the off-shell effects is to cure an undesirable increase in the predicted photoproduction total cross-section above roughly 1.5 GeV. By examining the non-pole part  $P_{ij}^{NP}$  of the amplitudes in Appendix B, one finds<sup>5</sup> that for the off-shell parameters  $X \neq -1/2$  and  $Z \neq 0$ , there are contributions to the invariant amplitudes which rise linearly as a function of the  $s$ -variable (observe that  $Y$  does not participate in this matter). Hence, the cross section increase stated above might be due to the  $X \neq -1/2$  and  $Z \neq 0$  values, as obtained from the present minimizations (Table I) exploiting the available data.

The authors of Ref. [5] have discussed extensively different "choices" of these free parameters, and especially fixing two of them, as reported in the literature [22]. They conclude that there is no physical basis to attribute fixed values to any of these off-shell parameters.

However, to numerically estimate the consequences of eliminating the undesirable  $s$ -dependent terms by imposing  $X = -1/2$  and  $Z = 0$ , we have performed a minimization within the context of model B. The results for the coupling constants and the only adjusted off-shell parameter ( $Y$ ) are given in Table I as model D. We see that the only significant variation compared to model B concerns the  $Y$ -parameter. Notice that for model B we had already  $Z \approx 0$ . Hence, decreasing the magnitude of the  $X$  parameter by roughly a factor

---

<sup>5</sup> From Eqs. B10 and B12 in Appendix B, we see that only three of the non-pole coefficients ( $P_{11}^{NP}$ ,  $P_{21}^{NP}$ , and  $P_{23}^{NP}$ ) depend on the  $s$  variable and that this dependence is linear. We write hence  $P_{ij}^{NP} = a_{ij}s + b_{ij}$ , where the coefficients  $a_{ij}$  and  $b_{ij}$  are functions of only off-shell parameters and baryons masses. Then one can readily derive the following expressions:

$a_{11} \propto (\tilde{Z} - 1/2)(2\tilde{Y} - 1)$ ;  $a_{21} \propto (\tilde{Z} - 1/2) + \tilde{X} [1 - 2\tilde{Z}(M_Y/M_R + 2)]$ ;  $a_{23} \propto \tilde{X}(\tilde{Z} - 1/2)$ . All these coefficients vanish at  $\tilde{X} = 0$  and  $\tilde{Z} = 1/2$  (i.e.,  $X = -1/2$  and  $Z = 0$ ).

of 2 (between models B and D) leads to an increase of about 20% of the magnitude of the  $Y$ -parameter. In Figure 8 the photoproduction total cross section and the electroproduction ratio  $R(t) = d\sigma_L/d\sigma_U$  are depicted for both B and D models. In both cases the results from the two models are quite close and the photoproduction total cross section comes out to give slightly higher values using the *ad hoc* fixed values for  $X$  and  $Z$  [Fig. 8(a)]. Other observables discussed in this paper show similar behaviors while comparing models B and D. The closeness of the predictions for the observables can be understood by noticing that the  $Z$  parameter in model B has a value compatible with zero, and the contributions due to the  $Y$ -dependent terms dominate numerically over those coming from the  $Z$ -dependent ones.

In the case of pion photoproduction, the RPI-group [6] found that imposing  $X = -1/2$  and  $Z = 0$  leads to a significant increase of the  $\chi^2$ . This is not the case with the present investigation (Table I). The reason is that the pion photoproduction was studied in the  $\Delta_{33}$  resonance region, where the reaction mechanism is dominated by this spin-3/2 resonance, while in the case of strangeness production none of the resonances has a paramount role. Moreover, we recall that the model B (C) studied here contains one (two) spin-3/2 resonance and five spin-1/2 resonances.

To our knowledge, there are *a priori* no bounds on the values of the off-shell parameters. However, remembering that the off-shell freedom comes in only from the non-pole terms, and that the principal contribution from a given resonance must correspond to the propagation of its proper spin, we expect that the corresponding non-pole parts might not dominate the pole part. This would give reasonable upper-bound to which values  $X$ ,  $Y$ , and  $Z$  may take. This expectation was verified in the case of the models reported here.

Finally, in the case of  $L8$  hyperonic resonance (model C), very small values of the off-shell parameters, as well as those of coupling constants resulting from the minimization endorse our previous affirmations: contributions from this resonance are not required by the existing data base, and the smallness of the relevant free parameters explains why its inclusion in the underlying dynamics does not have significant consequences, neither on the  $\chi^2$  nor on the predicted observables.

## V. SUMMARY AND CONCLUSIONS

In the present article, focused on the electromagnetic production of strangeness, we have been concerned with the improvement on the effective hadronic Lagrangian approaches by incorporating the correct spin-3/2 resonances propagators and what is called off-shell effects entering the vertices connected to these resonances.

The work presented here allows us to preserve the gauge invariance of the formalism, to ensure that each propagator associated with a spin-3/2 exchanged baryon has an inverse, and to include simultaneously both  $N^*$  and  $Y^*$  spin-3/2 resonances.

Applying our approach to the  $K\Lambda$  channels observables investigated in Ref [1], we have emphasized that the photo- and electro-production of  $K^+\Lambda$  observables show significant sensitivity to the off-shell effects, while these effects do not lead to measurable manifestations in the  $K^-p$  radiative capture branching ratio with stopped kaons.

The numerical results reported here are of course heavily based on the existing data. Given the inconsistencies [11] within the present data, the dynamical content of the models reported here will very likely evolve with the forthcoming high quality data from several experiments, both ongoing and planned. Hence the presented numerical results should be considered as guidelines for relative effects. The efforts in refining the phenomenological approaches are then meant to provide us with appropriate tools to interpret the upcoming data.

Applying the formalism derived in this paper to the available data-base, our results show that the photoproduction data, especially polarization asymmetries, are crucial in pinning down the role of off-shell effects. Once these effects are under control, the electroproduction channel can be investigated in studying the electromagnetic form factors of the baryons, kaon and their resonances. These conclusions were reached for the  $K\Lambda$  channels and we are currently investigating the complementary  $K\Sigma$  processes.

There are a few items not discussed in our investigation here for which some comments may be due.

In none of the reported approaches (including this work) the constructed amplitudes embody unitarity. Recently, there has been some attempts to unitarize the amplitude in this process. Lu *et al.* [23] have performed a “*feasibility study*” within a chiral color dielectric model adopting a simple two-channel case and using the  $K^+N$  phase shifts to approximate the  $K^+\Lambda$  elastic scattering in the final state. Kaiser *et al.* [24] have developed an SU(3)



chiral dynamics with an effective coupled-channel potential. This  $s$ -wave approximation approach is limited to the near threshold region. These works put forward some indications on the effects from the unitarization, but they do not offer a definitive conclusion about the importance of the final state interactions.

When several final channels are taken into account, to be realistic, a complete unitarization procedure becomes beyond our current capacity. Note also that there has not been any unique way the unitarization should be carried on. We thus believe and hope that, since the finite widths of the resonances are included, some parts contributing towards unitarization have been effectively included in the models discussed in this paper.

Before ending this Section, we wish to discuss briefly two recent and more fundamental approaches applied to some of the processes investigated in this paper.

(i) *Chiral Perturbation Theory (CHPT)*: This approach *limited to the threshold region*, incorporates the coupling to baryon multiplets, as has recently been done in Ref. [25] putting more emphasis on the consequence from the strict chiral symmetry in the construction of Lagrangian. Here we simply note that the predictions of this model reproduce reasonably the low energy total photoproduction cross sections and the recoil polarization  $P$ , and are qualitatively consistent with our results. To establish the quality of the *CHPT* predictions extended to three flavors and including baryons, more data near threshold are needed.

(ii) *Quark Models*: These models (upon adopting some type of chiral quark model, for example Ref. [26]) can predict certain observables with less number of free parameters than the Effective Hadronic Lagrangian (EHL) approaches, given the consequence of the difference in the underlying quark models is well within some controllable limit. Right now *the electroproduction process is rather hard to deal with* by the existing quark model approaches to the strangeness production.

We observe that in the current stage of development, the Quarks models and the EHL approaches are somewhat complementary. With available data and upon minimization, EHL can supply the values of combined coupling constants like  $G_1$  and  $G_2$  in our present approach. Then, the thus obtained amplitudes are able to predict yet unmeasured observables. Once those observables are measured, they will serve in constraining the hadronic coupling values. They are then decomposed into pure hadronic and strong-electromagnetic parts, to constrain the underlying sub-hadronic dynamics (selecting certain quark models, for example).

Some quantities are present in one approach which are absent in the other (like the off-shell effects). We still lack a microscopic covariant approach within quark models which

could, in principle, answer questions related to these aspects.

Concluding, the complementarity between the Effective Lagrangian approach and other promising investigations [23–26], provide us with powerful theoretical means to interpret the copious and high quality data to come.

### **ACKNOWLEDGMENTS**

We would like to thank Jean-Christophe David, Zhenping Li and Nimai Mukhopadhyay for fruitful discussions, and Dietmar Menze and Reinhard Schumacher for helpful exchanges on the experimental results and projects.

## APPENDIX A:

### CGLN amplitudes

The well-known Chew, Goldberger, Low and Nambu (*CGLN*) amplitudes entering into the expressions of the photo- and electro-production observables (see for example Ref. [1]) are related to the  $\mathcal{A}_j$  invariant functions as follows:

$$\mathcal{F}_1 = (\sqrt{s} - M_p)\mathcal{A}_1 - p_\gamma \cdot p_p \mathcal{A}_3 - p_\gamma \cdot p_Y \mathcal{A}_4 - p_\gamma^2 \mathcal{A}_5, \quad (\text{A1})$$

$$\mathcal{F}_2 = \frac{|\mathbf{p}_\gamma||\mathbf{p}_K|}{(E_p + M_p)(E_Y + M_Y)} \left[ (\sqrt{s} + M_p)\mathcal{A}_1 + p_\gamma \cdot p_p \mathcal{A}_3 + p_\gamma \cdot p_Y \mathcal{A}_4 + p_\gamma^2 \mathcal{A}_5 \right], \quad (\text{A2})$$

$$\mathcal{F}_3 = \frac{|\mathbf{p}_\gamma||\mathbf{p}_K|}{(E_p + M_p)} \left[ -2p_\gamma \cdot p_p \mathcal{A}_2 + (\sqrt{s} + M_p)\mathcal{A}_4 + p_\gamma^2 \mathcal{A}_6 \right], \quad (\text{A3})$$

$$\mathcal{F}_4 = \frac{|\mathbf{p}_K|^2}{(E_Y + M_Y)} \left[ 2p_\gamma \cdot p_p \mathcal{A}_2 + (\sqrt{s} - M_p)\mathcal{A}_4 - p_\gamma^2 \mathcal{A}_6 \right], \quad (\text{A4})$$

$$\mathcal{F}_5 = \frac{|\mathbf{p}_\gamma|^2}{(E_p + M_p)} \left[ -\mathcal{A}_1 + 2p_\gamma \cdot p_Y \mathcal{A}_2 + (\sqrt{s} + M_p)(\mathcal{A}_3 - \mathcal{A}_5) + (p_\gamma \cdot p_Y - p_\gamma \cdot p_p - p_\gamma^2)\mathcal{A}_6 \right], \quad (\text{A5})$$

$$\mathcal{F}_6 = \frac{|\mathbf{p}_\gamma||\mathbf{p}_K|}{(E_Y + M_Y)} \left[ -2p_\gamma \cdot p_Y \mathcal{A}_2 + (\sqrt{s} - M_p)\mathcal{A}_3 - (p_\gamma \cdot p_Y - p_\gamma \cdot p_p - p_\gamma^2)\mathcal{A}_6 - \right. \quad (\text{A6})$$

$$\left. \frac{1}{E_p + M_p} \left\{ p_{\gamma 0} \mathcal{A}_1 + p_\gamma \cdot p_p \mathcal{A}_3 + p_\gamma \cdot p_Y \mathcal{A}_4 + p_{\gamma 0} (\sqrt{s} + M_p) \mathcal{A}_5 \right\} \right]. \quad (\text{A7})$$

The only differences with the relations given in Appendix D of Ref [1] appear in the amplitudes  $\mathcal{F}_5$  and  $\mathcal{F}_6$  (contributing only in the electroproduction observables) where we have the following extra term inside the braces:  $-(p_\gamma \cdot p_p + p_\gamma^2)\mathcal{A}_6$ .

## APPENDIX B:

### Invariant amplitudes from an $s$ -channel spin 3/2 resonance

Here we present the concrete form for the invariant amplitudes decomposed into the pole (P) and non-pole (NP) parts as discussed in Eqs. (2.25) to (2.27). The calculation has been done both manually, and by using MAPLE to confirm the validity of the former.

To begin, we first introduce several coefficients as well as a few Lorentz scalar products which enter the expressions for the amplitudes.

$$A = -\frac{1}{6 M_R^2} (M_Y^2 + M_R^2 - M_K^2 - M_R M_Y), \quad (\text{B1})$$

$$B(\tilde{Z}) = \frac{1 - 2\tilde{Z}}{6 M_R^2}, \quad (\text{B2})$$

$$C = \frac{1}{12 M_R^2 (p_\gamma \cdot p_Y - p_\gamma \cdot p_p)} \left[ 2 M_R M_p M_Y - (M_Y^2 + M_R^2 - M_K^2) (2 M_p - 3 M_R) \right], \quad (\text{B3})$$

$$D(\tilde{X}, \tilde{Z}) = \frac{1}{12 M_R^2 (p_\gamma \cdot p_Y - p_\gamma \cdot p_p)} \left[ (2 M_p - M_R) - 2 (M_R + 2 M_Y + 2 M_p) \tilde{Z} \right. \\ \left. - 2 M_R \tilde{X} + 4 (M_Y + 2 M_R) \tilde{X} \tilde{Z} \right], \quad (\text{B4})$$

$$E = \frac{1}{12 M_R} \left[ M_K^2 - (M_Y + M_R)^2 \right], \quad (\text{B5})$$

$$F(\tilde{X}, \tilde{Z}) = \frac{1}{12 M_R^2} \left[ M_R - 2 M_R \tilde{Z} - 2 M_R \tilde{X} + 4 (M_Y + 2 M_R) \tilde{X} \tilde{Z} \right]. \quad (\text{B6})$$

The dot products are given by

$$p_\gamma \cdot p_p = \frac{1}{2} (s - M_p^2 - p_\gamma^2) \quad , \quad p_\gamma \cdot p_Y = \frac{1}{2} (M_Y^2 + p_\gamma^2 - u), \quad (\text{B7})$$

Using the relation  $s + t + u = M_p^2 + M_Y^2 + M_K^2 + p_\gamma^2$ , we obtain

$$p_\gamma \cdot p_Y - p_\gamma \cdot p_p = \frac{1}{2} (t - M_K^2 - p_\gamma^2), \quad (\text{B8})$$

With this preparation above we first present the quantities  $P_{1j}^{P,NP}$  ( $j = 1, \dots, 4$ ) for the photoproduction coming from the  $G_1$  coupling

$$P_{11}^P = \left( \frac{1}{6} \frac{M_p^2}{M_R^2} - \frac{1}{3} \frac{M_p}{M_R} - \frac{1}{2} \right) M_Y^2 + \left( -\frac{1}{6} \frac{M_p^2}{M_R} - \frac{2}{3} M_p - \frac{1}{2} M_R \right) M_Y \\ + \left( -\frac{1}{3} - \frac{1}{6} \frac{M_K^2}{M_R^2} \right) M_p^2 + \left( -\frac{1}{3} M_R + \frac{1}{3} \frac{M_K^2}{M_R} \right) M_p + \frac{1}{2} t,$$

$$P_{12}^P = 1,$$

$$P_{13}^P = \frac{1}{3} \frac{M_Y^2 M_p}{M_R^2} + \left( -\frac{1}{3} \frac{M_p}{M_R} - 1 \right) M_Y + \left( \frac{1}{3} - \frac{1}{3} \frac{M_K^2}{M_R^2} \right) M_p,$$

$$P_{14}^P = -(M_p + M_R),$$

(B9)

$$\begin{aligned}
P_{11}^{NP} &= \frac{2}{3} \frac{(s + M_Y M_p + 2 M_R M_Y + 2 M_R M_p) \tilde{Y} \tilde{Z}}{M_R^2} \\
&\quad - \frac{1}{3} \frac{(s - M_Y^2 + M_R M_Y + M_R M_p + M_K^2) \tilde{Y}}{M_R^2} \\
&\quad + \frac{1}{3} \frac{(-s - 2 M_R M_Y + M_p^2 - 2 M_R M_p) \tilde{Z}}{M_R^2} \\
&\quad - \frac{1}{6} \frac{-s + M_Y^2 - M_R M_Y + M_p^2 - 2 M_R M_p - M_K^2}{M_R^2}, \\
P_{12}^{NP} &= 0, \\
P_{13}^{NP} &= \frac{4}{3} \frac{(M_Y + 2 M_R) \tilde{Y} \tilde{Z}}{M_R^2} - \frac{2}{3} \frac{\tilde{Y}}{M_R} + \frac{2}{3} \frac{(-M_Y + M_p - 2 M_R) \tilde{Z}}{M_R^2} \\
&\quad - \frac{1}{3} \frac{M_p - M_R}{M_R^2}, \\
P_{14}^{NP} &= 0.
\end{aligned} \tag{B10}$$

Those coming from the  $G_2$  coupling, viz.  $P_{2j}^{P,NP}$  ( $j=1,\dots,4$ ) are

$$\begin{aligned}
P_{21}^P &= -E (M_R^2 - M_p^2), \\
P_{22}^P &= \frac{1}{2} (M_p - M_R), \\
P_{23}^P &= -\frac{1}{6} \frac{(M_Y + 2 M_R) (M_p - M_R) M_Y}{M_R} + \frac{1}{2} M_p^2 + \frac{1}{6} \frac{(M_K^2 - M_R^2) (M_p + 2 M_R)}{M_R} - \frac{1}{2} t, \\
P_{24}^P &= -\frac{1}{2} (M_p^2 - M_R^2),
\end{aligned} \tag{B11}$$

$$\begin{aligned}
P_{21}^{NP} &= -E - F(\tilde{X}, \tilde{Z}) (s - M_p^2), \\
P_{22}^{NP} &= 0, \\
P_{23}^{NP} &= \frac{2}{3} \frac{(-s + M_Y M_p - 2 M_R M_Y + 2 M_R M_p) \tilde{X} \tilde{Z}}{M_R^2} \\
&\quad - \frac{1}{3} \frac{(-s + M_Y^2 - M_R M_Y + M_R M_p - M_K^2) \tilde{X}}{M_R^2} - \frac{1}{3} \frac{(-M_Y + M_p) \tilde{Z}}{M_R} \\
&\quad + \frac{1}{6} \frac{M_p - 2 M_R}{M_R}, \\
P_{24}^{NP} &= \frac{1}{2}.
\end{aligned} \tag{B12}$$

The parts for  $j = 1, \dots, 4$  contributing to the electroproduction [see Eq. (2.27)] are as follows:

- those related to coupling  $G_1$

$$\begin{aligned}
R_{11}^P &= A \quad , \quad R_{12}^P = \frac{2A - 1}{2(p_\gamma \cdot p_Y - p_\gamma \cdot p_p)}, \\
R_{13}^P &= R_{14}^P = 0, \\
R_{11}^{NP} &= B(\tilde{Z}) \quad , \quad R_{12}^{NP} = \frac{B(\tilde{Z})}{p_\gamma \cdot p_Y - p_\gamma \cdot p_p}, \\
R_{13}^{NP} &= R_{14}^{NP} = 0,
\end{aligned} \tag{B13}$$

- those related to coupling  $G_2$

$$\begin{aligned}
R_{21}^P &= E \quad , \quad R_{22}^P = C, \\
R_{23}^P &= -2A \quad , \quad R_{24}^P = -\frac{1}{2}, \\
R_{21}^{NP} &= F(\tilde{X}, \tilde{Z}) \quad , \quad R_{22}^{NP} = D(\tilde{X}, \tilde{Z}), \\
R_{23}^{NP} &= -2B(\tilde{Z}) \quad , \quad R_{24}^{NP} = 0.
\end{aligned} \tag{B14}$$

For  $j = 5, 6$  (contributing solely to the electroproduction) the  $E_{ij}$  coefficients coming from  $G_1$  are

$$\begin{aligned}
E_{15}^P &= -2A(M_R + M_p) \quad , \quad E_{16}^P = \frac{2A p_\gamma \cdot p_p - p_\gamma \cdot p_Y}{p_\gamma \cdot p_Y - p_\gamma \cdot p_p}, \\
E_{15}^{NP} &= -\frac{1}{3} \frac{M_p}{M_R^2} + \frac{2}{3} \frac{(-M_Y - M_R + M_p) \tilde{Z}}{M_R^2} - \frac{1}{3} \frac{\tilde{Y}}{M_R} + \frac{2}{3} \frac{(M_Y + 2M_R) \tilde{Y} \tilde{Z}}{M_R^2}, \\
E_{16}^{NP} &= \frac{2B(\tilde{Z}) p_\gamma \cdot p_p}{p_\gamma \cdot p_Y - p_\gamma \cdot p_p}.
\end{aligned} \tag{B15}$$

while those coming from  $G_2$  are

$$\begin{aligned}
E_{25}^P &= 2A p_\gamma \cdot p_p \quad , \quad E_{26}^P = 2C p_\gamma \cdot p_p, \\
E_{25}^{NP} &= 2B(\tilde{Z}) p_\gamma \cdot p_p \quad , \quad E_{26}^{NP} = 2D(\tilde{X}, \tilde{Z}) p_\gamma \cdot p_p.
\end{aligned} \tag{B16}$$

## APPENDIX C:

### Vertices adopted by Adelseck *et al.*

Here we show how the vertices Eqs. (2.21) and (2.22) may be reduced, by some assumption and approximation, to the ones used by Adelseck *et al.* [3].

As discussed in [5], the propagator adopted by Adelseck *et al.* Eq. (2.30) may be rewritten (*in the limit of zero width*) as

$$P_{\mu\nu}^A(q) = \frac{\not{q} + \sqrt{s}}{s - M_R^2} \mathcal{P}_{\mu\nu}^{3/2}(q), \quad (\text{C1})$$

where  $\mathcal{P}_{\mu\nu}^{3/2}(q)$  is the projection operator for spin 3/2 states. Thus this choice of the propagator cuts out the propagation of spin 1/2 states. With this the scattering amplitude Eq. (2.20) reads

$$M_{fi}^{(s)} = \bar{U}_Y(\mathbf{p}_Y) \mathcal{V}^\mu(KYR) \frac{\not{q} + \sqrt{s}}{s - M_R^2 + i\Gamma_R M_R} \mathcal{P}_{\mu\nu}^{3/2}(q) \mathcal{V}^\nu(Rp\gamma) U_p(\mathbf{p}_p). \quad (\text{C2})$$

For an on-mass-shell positive energy resonance the spin 3/2 projection operator may be written as

$$\mathcal{P}_{\mu\nu}^{3/2}(q) = \sum U_\mu(\mathbf{q}) \bar{U}_\nu(\mathbf{q}), \quad (\text{C3})$$

where the summation is implied over the spin eigenstates.

By assuming that the propagating spin 3/2 resonance is approximately on-mass-shell, and in a positive energy state, we find

$$M_{fi}^{(s)} \approx \sum \bar{U}_Y(\mathbf{p}_Y) \mathcal{V}^\mu(KYR) U_\mu(\mathbf{q}) \frac{\sqrt{s} + M_R}{s - M_R^2 + i\Gamma_R M_R} \bar{U}_\nu(\mathbf{q}) \mathcal{V}^\nu(Rp\gamma) U_p(\mathbf{p}_p). \quad (\text{C4})$$

In the above expression the equation

$$(\not{q} - M_R) U_\mu(\mathbf{q}) = 0, \quad (\text{C5})$$

has been used. So by this assumption (or approximation), we have only to find out the structure of (by suppressing the index for spin eigenstates) the following matrix elements

$$\bar{U}_Y(\mathbf{p}_Y) \mathcal{V}^\mu(KYR) U_\mu(\mathbf{q}), \quad (\text{C6})$$

and

$$\bar{U}_\nu(\mathbf{q})\mathcal{V}^\nu(Rp\gamma)U_p(\mathbf{p}_p). \quad (\text{C7})$$

First, by disregarding the off-shell freedom, the  $KYR$  vertex in Eq. (2.21), upon sandwiched between two spinors Eq. (C6), becomes

$$\bar{U}_Y(\mathbf{p}_Y)\mathcal{V}^\mu(KYR)U_\mu(\mathbf{q}) = \frac{g_{KYR}}{M_K}p_Y^\mu\bar{U}_Y(\mathbf{p}_Y)U_\mu(\mathbf{q}), \quad (\text{C8})$$

which results from

$$q^\mu U_\mu(\mathbf{q}) = (p_K + p_Y)^\mu U_\mu(\mathbf{q}) = 0. \quad (\text{C9})$$

This is a consequence from one of the constraints for spin 3/2 field  $R_\mu$ , recall Section II.A:  $\partial^\mu R_\mu = 0$ .

Thus by introducing  $\tilde{g}_{KYR}$  through

$$\frac{\tilde{g}_{KYR}}{M_R} \equiv \frac{g_{KYR}}{M_K}, \quad (\text{C10})$$

we may identify the  $KYR$  vertex of Adelseck *et al.* as

$$\mathcal{V}^\mu(KYR) \approx \frac{\tilde{g}_{KYR}}{M_R}p_Y^\mu. \quad (\text{C11})$$

We now look at the  $Rp\gamma$  vertex whose matrix element is defined in Eq. (C7). With no off-shell freedom implemented, the vertex Eq. (2.22) reads

$$\mathcal{V}^\nu(Rp\gamma) = \left[ \frac{eg_1}{2M_p}(\epsilon^\nu \not{p}_\gamma - p_\gamma^\nu \not{\epsilon}) + \frac{eg_2}{4M_p^2}(\epsilon \cdot p_p p_\gamma^\nu - p_\gamma \cdot p_p \epsilon^\nu) \right] i\gamma^5. \quad (\text{C12})$$

The second term in the large bracket can be handled quite easily: even without taking its matrix element, we can simply define the coupling constant  $g_b$  through

$$\frac{g_b}{(M_R + M_p)^2} \equiv \frac{eg_2}{4M_K^2}. \quad (\text{C13})$$

Next, to find  $g_a$  we take the matrix element of the first term in the large bracket of Eq. (C12), that is proportional to  $g_1$ . This reads

$$i\frac{eg_1}{2M_p}\bar{U}_\nu(\mathbf{q})(\epsilon^\nu \not{p}_\gamma - p_\gamma^\nu \not{\epsilon})\gamma^5 U(\mathbf{p}_p). \quad (\text{C14})$$

Then we exploit the following relations

$$p_\gamma = q - p_p, \quad (\text{C15})$$

$$\not{p}_\gamma \gamma^5 U(\mathbf{p}_p) = -M_p \gamma^5 U(\mathbf{p}_p), \quad (\text{C16})$$

$$\bar{U}_\nu(\mathbf{q})\not{\epsilon} = \bar{U}_\nu(\mathbf{q})M_R. \quad (\text{C17})$$



Then Eq. (C14) may be rewritten as

$$eg_1 \frac{(M_R + M_p)}{2M_p} \bar{U}_\nu(\mathbf{q}) \left[ \epsilon^\nu - \frac{p_\gamma^\nu}{M_R + M_p} \not{\epsilon} \right] i\gamma^5 U(\mathbf{p}_p). \quad (\text{C18})$$

Thus by defining  $g_a$  through

$$\frac{g_a}{M_R + M_p} \equiv \frac{eg_1}{2M_p}, \quad (\text{C19})$$

the Eq. (C18) reads

$$\bar{U}_\nu(\mathbf{q}) g_a \left[ \epsilon^\nu - \frac{p_\gamma^\nu}{M_R + M_p} \not{\epsilon} \right] U(\mathbf{p}_p). \quad (\text{C20})$$

Then everything put together, the  $Rp\gamma$  vertex becomes

$$\mathcal{V}^\nu(Rp\gamma) \approx i \left[ g_a \left( \epsilon^\nu - \frac{p_\gamma^\nu \not{\epsilon}}{M_R + M_p} \right) + g_b \frac{1}{(M_R + M_p)^2} (\epsilon \cdot p_p p_\gamma^\nu - p_\gamma \cdot p_p \epsilon^\nu) \right] \gamma^5. \quad (\text{C21})$$

A trouble with this form is that it does not respect gauge invariance. Thus in [3] the replacement  $M_R \rightarrow \sqrt{s}$  was made, which eventually leads to Eq. (2.32).

## REFERENCES

- [1] J. C. David, C. Fayard, G. H. Lamot, and B. Saghai, *Phys. Rev. C* **53**, 2613 (1996).
- [2] F. M. Renard and Y. Renard, *Nucl. Phys.* **B25**, 490 (1971); Y. Renard, *ibid.* **B40**, 499 (1972); Y. Renard, Thèse de Doctorat d'Etat ès-Sciences Physiques, Université des Sciences et Techniques du Languedoc, 1971 (in French).
- [3] R. A. Adelseck and L. E. Wright, *Phys. Rev. C* **38**, 1965 (1988); R. A. Adelseck, Ph.D. Thesis, Ohio University, 1988.
- [4] R. A. Adelseck, C. Bennhold, and L. E. Wright, *Phys. Rev. C* **32**, 1681 (1985).
- [5] M. Benmerrouche, R. M. Davidson, and Nimai C. Mukhopadhyay, *Phys. Rev. C* **39**, 2339 (1989).
- [6] R. M. Davidson, Nimai C. Mukhopadhyay, and R. S. Wittman *Phys. Rev. D* **43**, 71 (1991).
- [7] M. Benmerrouche, Nimai C. Mukhopadhyay, and J. F. Zhang, *Phys. Rev. D* **51**, 3237 (1995).
- [8] M. Benmerrouche, PhD Thesis, Rensselaer Polytechnic Institute (1992); Nimai C. Mukhopadhyay, J. F. Zhang, and M. Benmerrouche, Proceedings of the *Forth CE-BAF/INT Workshop on N\* Physics*, Seattle, WA, 9-13 Sept. 1996, Editors: T.-S. H. Lee and W. Roberts, (World Scientific, 1997).
- [9] J. D. Bjorken and S. D. Drell, *Relativistic Quantum Mechanics* (McGraw-Hill, New York, 1964).
- [10] B. Saghai and F. Tabakin, *Phys. Rev. C* **55**, 917 (1997).
- [11] R. A. Adelseck and B. Saghai, *Phys. Rev. C* **42**, 108 (1990).
- [12] R. A. Williams, C. R. Ji, and S. R. Cotanch, *Phys. Rev. C* **46**, 1617 (1992).
- [13] M. Bockhorst *et al.*, *Z. Phys.* **C 63**, 37 (1994).
- [14] P. L. Donoho and R. L. Walker, *Phys. Rev.* **112**, 981 (1958); B. D. McDaniel *et al.*, *ibid* **115**, 1039 (1959); H. M. Brody *et al.*, *ibid* **119**, 1710 (1960); R. L. Anderson *et al.*, *Phys. Rev. Lett.* **9**, 131 (1962); H. Thom *et al.*, *ibid* **11**, 434 (1963); C. W. Peck, *Phys. Rev.* **135**, 830 (1964); R. L. Anderson *et al.*, *Proc. Int. Symp. on electron and photon interactions at high energies*, Hamburg, (1965); S. Mori, Ph.D. Thesis, Cornell University (1966); H. Thom, *Phys. Rev.* **151**, 1322 (1966); D. E. Groom and J. H. Marshall, *ibid* **159**, 1213 (1967); R. Erbe *et al.*, *ibid* **188**, 2060 (1969); A. Bleckmann *et al.*, *Z. Phys.* **239**, 1 (1970); T. Fujii *et al.*, *Phys. Rev. D* **2**, 439 (1970); D. Decamp *et al.*, Orsay Report, LAL 1236 (1970); Th. Fourneron, Thèse de Doctorat d'Etat, Université

- de Paris, Report LAL 1258, 1971, (in French); H. Goeing *et al.*, Nucl. Phys. **B26**, 121 (1971); P. Feller *et al.*, *ibid* **B39**, 413 (1972).
- [15] B. Borgia *et al.*, Nuovo Cimento **32**, 218 (1964); M. Grilli *et al.*, *ibid* **38**, 1467 (1965); D. E. Groom and J. H. Marshall, Phys. Rev. **159**, 1213 (1967); R. Hass *et al.*, Nucl. Phys. **B137**, 261 (1978).
- [16] K. H. Althoff *et al.*, Nucl. Phys. **B137**, 269 (1978).
- [17] C. N. Brown *et al.*, Phys. Rev. Lett. **28**, 1086, (1972); T. Azemoon *et al.*, Nucl. Phys. B **95**, 77 (1975); C. J. Bebek *et al.*, Phys. Rev. D **15**, 594 (1977); *ibid.* D **15**, 3082 (1977); P. Brauel *et al.*, Z. Phys. C **3**, 101 (1979).
- [18] SAPHIR Collaboration (J. Barth *et al.*) Contributed paper to the *6th Conference on the Intersections of Particle and Nuclear Physics* (CIPANP 97), Big Sky, MT, 27 May - 2 June 1997 (nucl-th/9707025); D. Menze, *private communication*.
- [19] C. R. Ji, and S. R. Cotanch, Phys. Rev. C **38**, 2691 (1988).
- [20] D. A. Whitehouse *et al.*, Phys. Rev. Lett. **63**, 1352 (1989).
- [21] B. Saghai and F. Tabakin, Phys. Rev. C **53**, 66 (1996).
- [22] L. M. Nath and B. Bhattacharyya, Z. Phys. C **5**, 9 (1980).
- [23] D. Lu, R. H. Landau, and S. C. Phatak, Phys. Rev. C **52**, 1662 (1995).
- [24] N. Kaiser, T. Waas, and W. Weise, Nucl. Phys. A **612**, 297 (1997).
- [25] S. Steininger and U.-G. Meißner, Phys. Lett. **B391**, 446 (1997).
- [26] Zhenping Li, Phys. Rev. C **52**, 1648 (1995); Zhenping Li, Hongxing Ye, and Minghui Lu, *ibid.* C **56**, 1099 (1997).

## TABLES

TABLE I. Exchanged particles, coupling constants, and off-shell parameters (*OSP*) for  $K\Lambda$  channels from models SL [1], and this work (A, B, and C). The reduced  $\chi^2$ 's are given in the last row. Model A is a simplified version of the SL model with  $N1$  (spin 1/2) and  $N8$  (spin 5/2) resonances removed. All the baryonic resonances have spin 1/2, except  $N7$  and  $L8$  (spin 3/2) for which off-shell treatment is applied (models B and C). Model D is identical to model B, with fixed values  $X = -1/2$ ,  $Z = 0$ , and  $Y$  free.

Notation	particle	$(\ell)J^\pi$	coupling and <i>OSP</i>	SL	A	B	C	D
	$\Lambda$	$\frac{1}{2}^+$	$g_{K\Lambda N}/\sqrt{4\pi}$	$-3.16 \pm 0.01$	$-3.16 \pm 0.01$	$-3.22 \pm 0.03$	$-3.22 \pm 0.01$	$-3.16 \pm 0.90$
	$\Sigma$	$\frac{1}{2}^+$	$g_{K\Sigma N}/\sqrt{4\pi}$	$0.91 \pm 0.10$	$0.78 \pm 0.08$	$0.83 \pm 0.10$	$0.86 \pm 0.02$	$0.87 \pm 0.06$
$K^{*+}$	$K^*(892)^+$	$1^-$	$G_V/4\pi$	$-0.05 \pm 0.01$	$-0.04 \pm 0.01$	$0.02 \pm 0.01$	$0.02 \pm 0.01$	$0.02 \pm 0.01$
			$G_T/4\pi$	$0.16 \pm 0.02$	$0.18 \pm 0.02$	$0.18 \pm 0.01$	$0.17 \pm 0.01$	$0.18 \pm 0.03$
$K1$	$K1(1270)$	$1^+$	$G_{V1}/4\pi$	$-0.19 \pm 0.01$	$-0.23 \pm 0.01$	$-0.15 \pm 0.01$	$-0.15 \pm 0.01$	$-0.17 \pm 0.01$
			$G_{T1}/4\pi$	$-0.35 \pm 0.03$	$-0.38 \pm 0.03$	$-0.38 \pm 0.04$	$-0.39 \pm 0.03$	$-0.35 \pm 0.03$
$N1$	$N(1440)$	$(1)\frac{1}{2}^+$	$G_{N1}/\sqrt{4\pi}$	$-0.01 \pm 0.12$				
$N7$	$N(1720)$	$(1)\frac{3}{2}^+$	$G_{N7}^1/4\pi$	$-0.04 \pm 0.01$	$-0.04 \pm 0.01$	$-0.04 \pm 0.01$	$-0.04 \pm 0.01$	$-0.03 \pm 0.01$
			$G_{N7}^2/4\pi$	$-0.14 \pm 0.04$	$-0.12 \pm 0.02$	$-0.10 \pm 0.01$	$-0.10 \pm 0.01$	$-0.11 \pm 0.02$
			X			$-1.03 \pm 0.21$	$-1.03 \pm 0.06$	$-0.5$
			Y			$8.25 \pm 0.28$	$8.19 \pm 0.12$	$9.84 \pm 0.19$
			Z			$0.003 \pm 0.014$	$10^{-5} \pm 0.01$	$0.$
$N8$	$N(1675)$	$(2)\frac{5}{2}^-$	$G_{N8}^a/4\pi$	$-0.63 \pm 0.10$				
			$G_{N8}^b/4\pi$	$-0.05 \pm 0.56$				
$L1$	$\Lambda(1405)$	$(0)\frac{1}{2}^-$	$G_{L1}/\sqrt{4\pi}$	$-0.31 \pm 0.06$	$-0.29 \pm 0.05$	$-0.28 \pm 0.02$	$-0.28 \pm 0.01$	$-0.29 \pm 0.05$
$L3$	$\Lambda(1670)$	$(0)\frac{1}{2}^-$	$G_{L3}/\sqrt{4\pi}$	$1.18 \pm 0.09$	$1.15 \pm 0.13$	$1.26 \pm 0.02$	$1.26 \pm 0.01$	$1.18 \pm 0.06$
$L5$	$\Lambda(1810)$	$(1)\frac{1}{2}^+$	$G_{L5}/\sqrt{4\pi}$	$-1.25 \pm 0.20$	$-3.89 \pm 1.45$	$-1.78 \pm 0.05$	$-1.78 \pm 0.02$	$-1.77 \pm 0.12$
$L8$	$\Lambda(1890)$	$(1)\frac{3}{2}^+$	$G_{L8}^1/4\pi$				$0.002 \pm 0.045$	
			$G_{L8}^2/4\pi$				$0.003 \pm 0.053$	
			X				$-0.02 \pm 3.92$	
			Y				$0.23 \pm 9.20$	
			Z				$0.23 \pm 9.00$	
$S1$	$\Sigma(1660)$	$(1)\frac{1}{2}^+$	$G_{S1}/\sqrt{4\pi}$	$-4.96 \pm 0.19$	$-2.43 \pm 1.20$	$-5.37 \pm 0.05$	$-5.36 \pm 0.02$	$-5.33 \pm 0.12$
$\chi^2$				1.73	1.84	1.66	1.69	1.66

TABLE II. Branching ratios ( $BR \times 10^3$  in Eq. [4.4]) for  $K^-p \rightarrow \gamma\Lambda$ , from the SL model and the present work (models A, B, C, D).

SL [1]	A	B	C	D	experiment [17]
0.95	1.00	0.99	0.99	1.00	$0.86 \pm 0.07 \pm 0.09$

## FIGURES

FIG. 1. Differential cross section for the process  $\gamma p \rightarrow K^+ \Lambda$ : excitation functions at  $\theta_K^{cm} = 27^\circ$  (a),  $90^\circ$  (b) and  $150^\circ$  (c), and angular distribution at  $E_\gamma^{lab} = 1.0$  GeV (d), 1.45 GeV (e), and 2.1 GeV (f). The curves are from models SL (dotted), A (dash-dotted), B (solid) and C (dashed). The SL model comes from Ref. [1], and model A is a simplified version of SL where the resonances  $N1$  and  $N8$  have been taken away (see Table I). Model B is the same as model A, but with off-shell effects for the only spin 3/2 resonance ( $N7$ ) in the reaction mechanism. Model C is the same as model B with an extra spin 3/2 (hyperonic) resonance ( $L8$ ), also with off-shell effects treatment. Data are from Refs. [10] (empty circles), and [11] (full circles).

FIG. 2. Total cross section for the reaction  $\gamma p \rightarrow K^+ \Lambda$  as a function of photon energy. Curves and data as in Fig. 1.

FIG. 3.  $\Lambda$ -polarization asymmetry ( $P$ ) in  $\gamma p \rightarrow K^+ \vec{\Lambda}$ , polarized target asymmetry ( $T$ ) in  $\vec{\gamma} p \rightarrow K^+ \Lambda$ , and linearly polarized beam asymmetry ( $\Sigma$ ) in  $\vec{\gamma} p \rightarrow K^+ \Lambda$ : excitation functions at  $\theta_K^{cm} = 90^\circ$  (a)-(c), and angular distributions at  $E_\gamma^{lab} = 1.45$  GeV (d)-(f) and  $E_\gamma^{lab} = 2.1$  GeV (g)-(i). Curves are as in Fig. 1, and data from Refs. [12] ( $P$ ), and [13] ( $T$ ).

FIG. 4. Angular distributions for double polarization asymmetries ( $C_{x'}$ ,  $C_{z'}$ ,  $O_{x'}$ , and  $O_{z'}$ ) in  $\vec{\gamma} p \rightarrow K^+ \vec{\Lambda}$  at  $E_\gamma^{lab} = 1.45$  GeV (a)-(d) and 2.1 GeV (e)-(h); curves as in Fig. 1.

FIG. 5. Differential cross section  $d\sigma_{UL}$  as a function of momentum transfer ( $Q^2$ ) for the reaction  $ep \rightarrow e' K^+ \Lambda$ , for  $W = 5.02$  GeV<sup>2</sup>,  $t = -0.15$  GeV<sup>2</sup>,  $\epsilon = 0.72$ . Curves are as in Fig. 1, and the data from Ref. [14].

FIG. 6. Same as Fig. 5, but for differential cross sections  $d\sigma_U(t)$ ,  $d\sigma_L(t)$ ,  $d\sigma_I(t)$ , and  $d\sigma_P(t)$ , see Eq. (4.1). Letters T and L stand for transverse and longitudinal, respectively, for  $W = 5.02$  GeV<sup>2</sup>,  $Q^2 = 1$  GeV<sup>2</sup>, and  $\epsilon = 0.72$ . Curves are as in Fig. 1.

FIG. 7. Same as Fig. 6, but for the longitudinal to transverse differential cross sections ratio  $R(t) = d\sigma_L/d\sigma_U$ . Curves are as in Fig. 1.

FIG. 8. (a) Total cross section for the reaction  $\gamma p \rightarrow K^+ \Lambda$  as a function of photon energy. (b) Longitudinal to transverse differential cross sections ratio  $R(t) = d\sigma_L/d\sigma_U$  for the reaction  $ep \rightarrow e' K^+ \Lambda$ . The curves are from models B (solid) and D (dashed). Model D has been obtained in the same conditions as model B, except that the off-shell parameters X and Z were fixed at  $-0.5$  and  $0.0$ , respectively (see Table I).

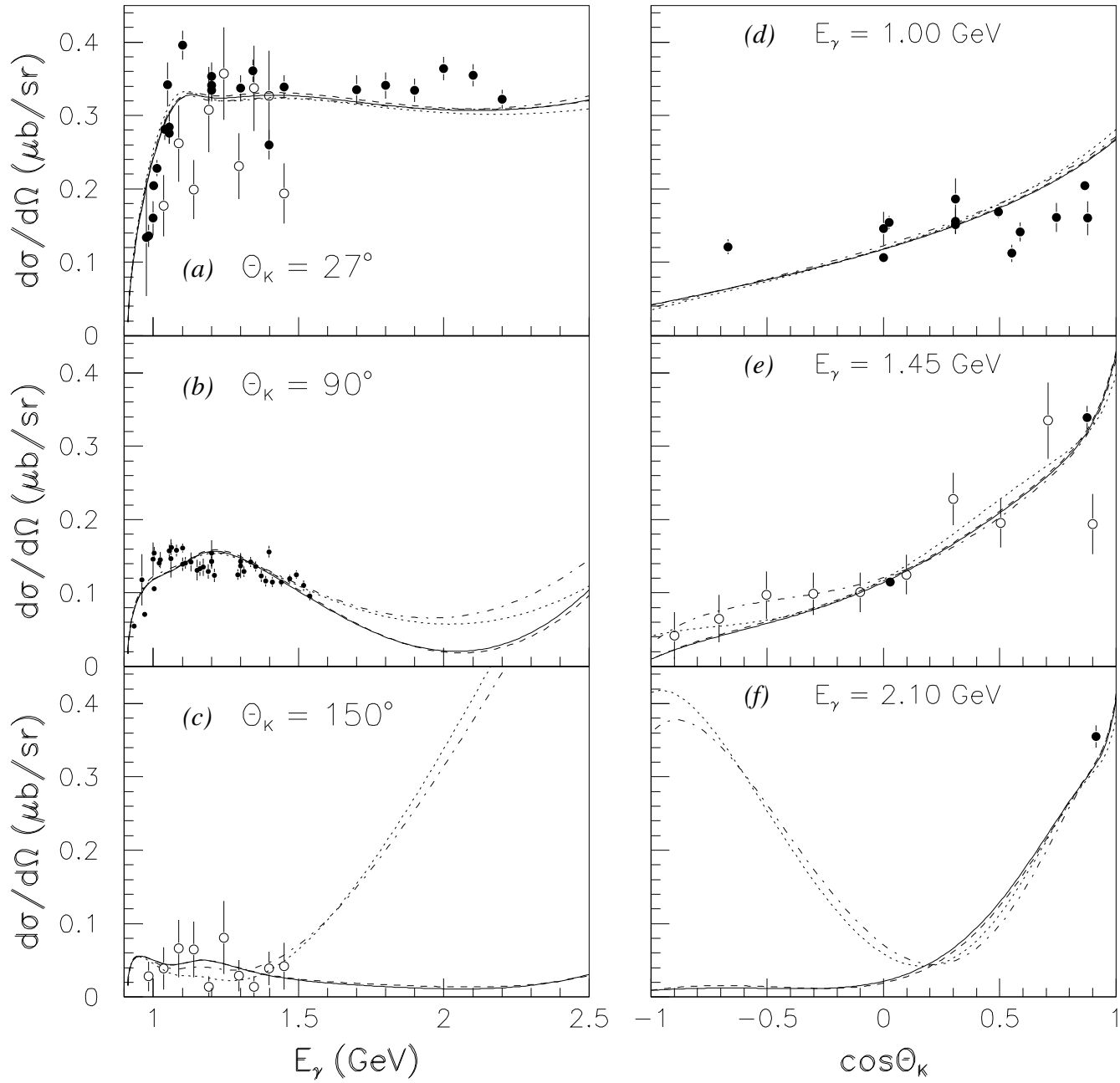


FIG. 1 - Mizutani et al., Off-shell effects...

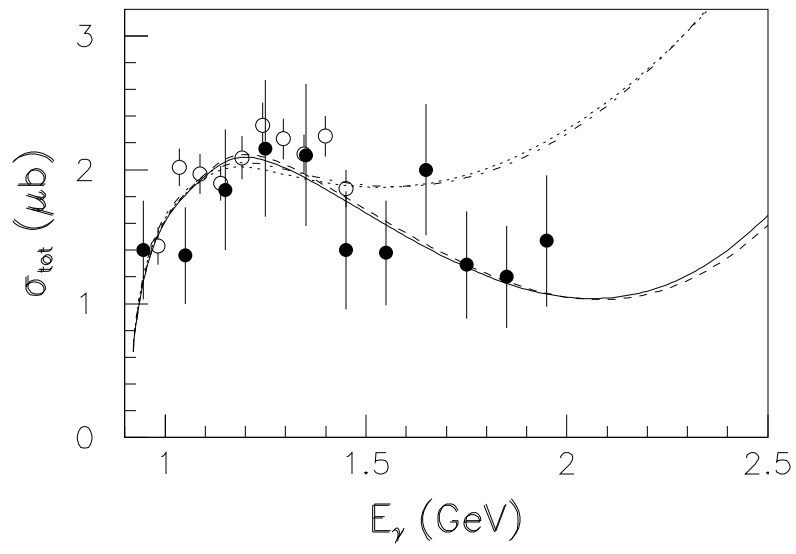


FIG. 2 - Mizutani et al., Off-shell effects...



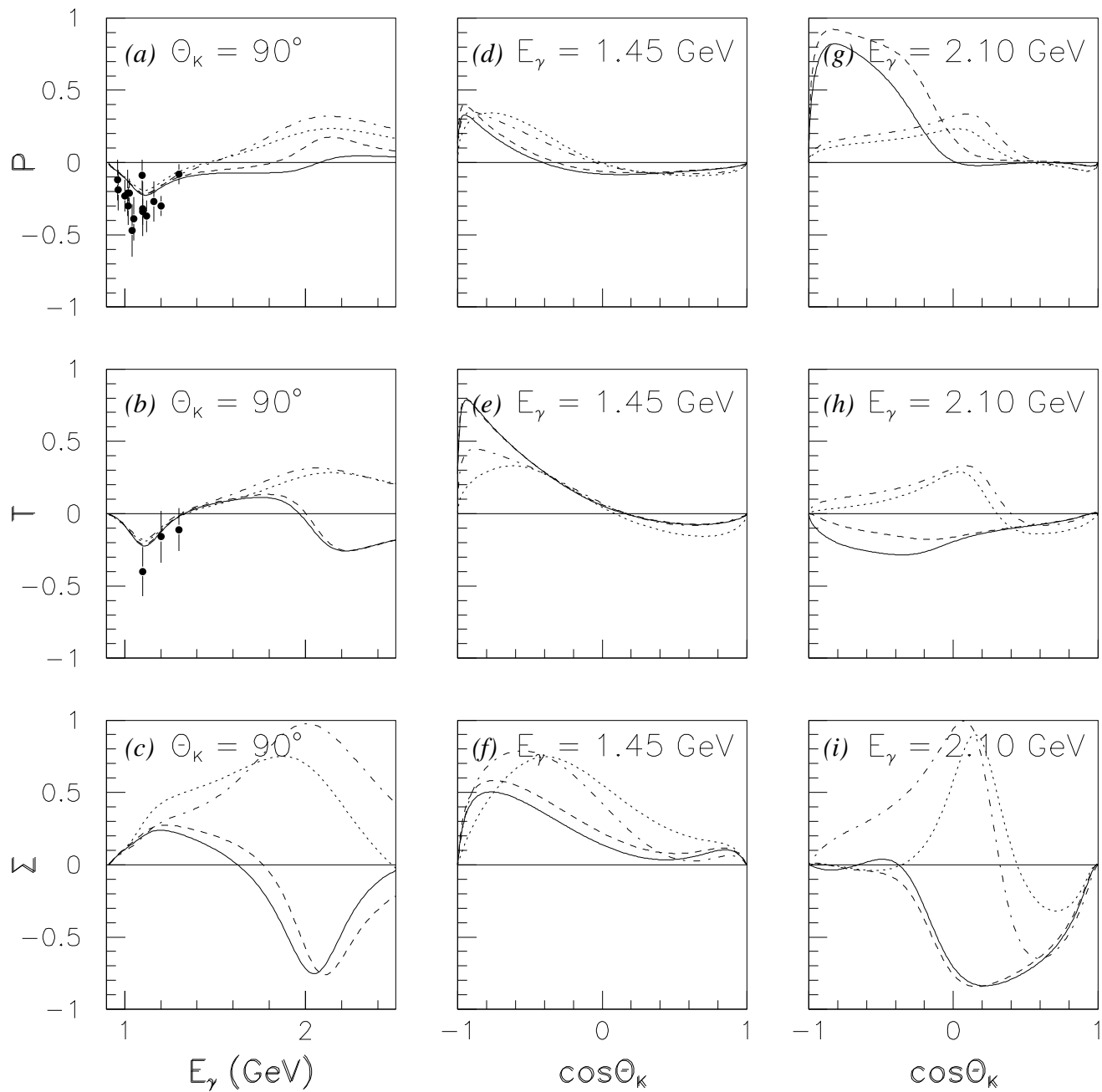
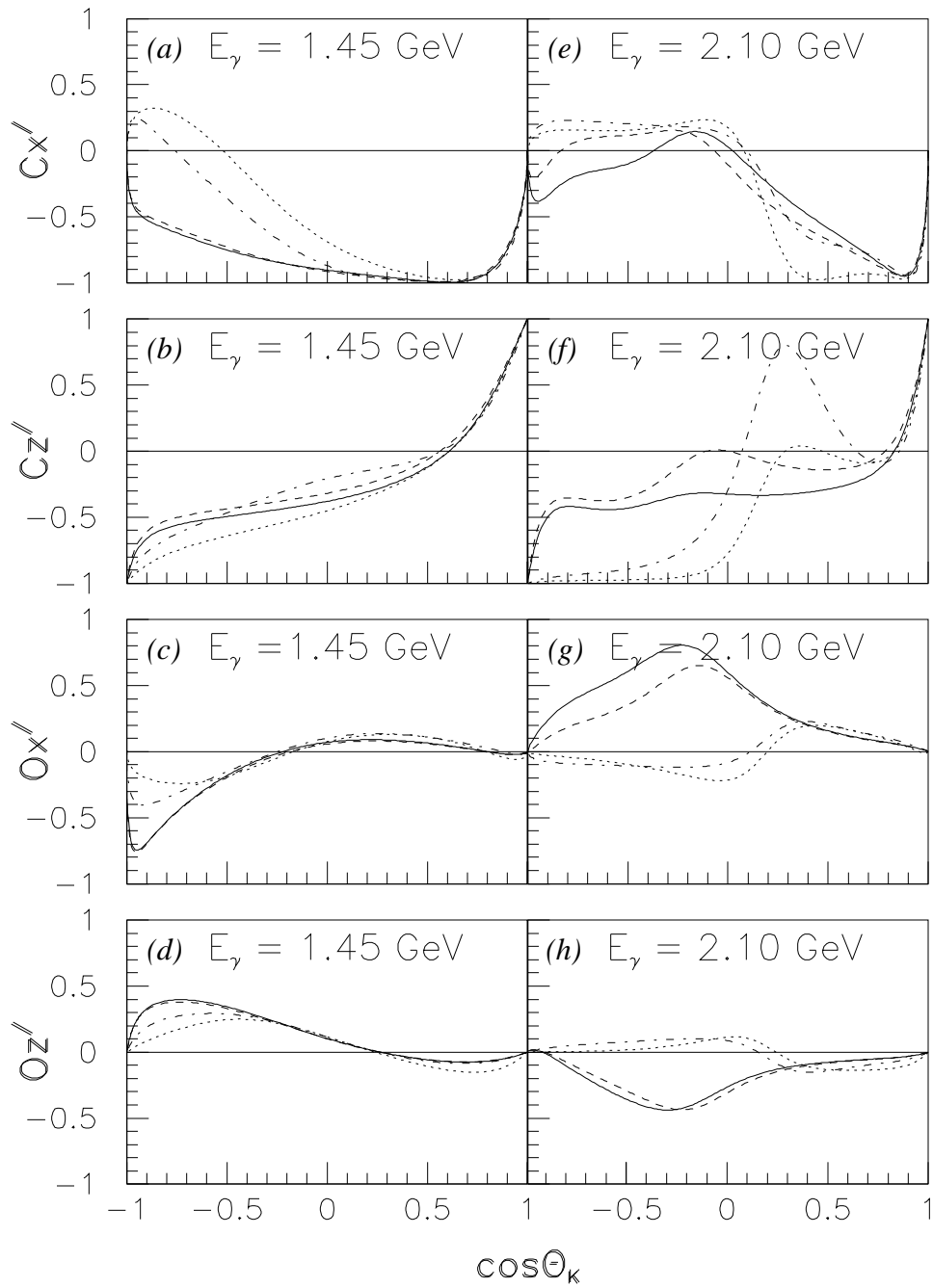
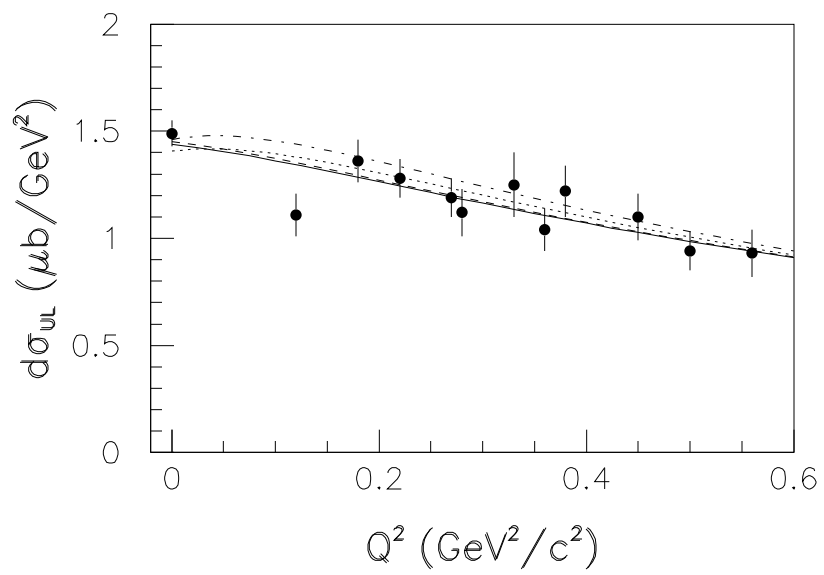


FIG. 3 - Mizutani et al., Off-shell effects...



**FIG. 4 - Mizutani et al., Off-shell effects...**



**FIG. 5 - Mizutani et al., Off-shell effects...**

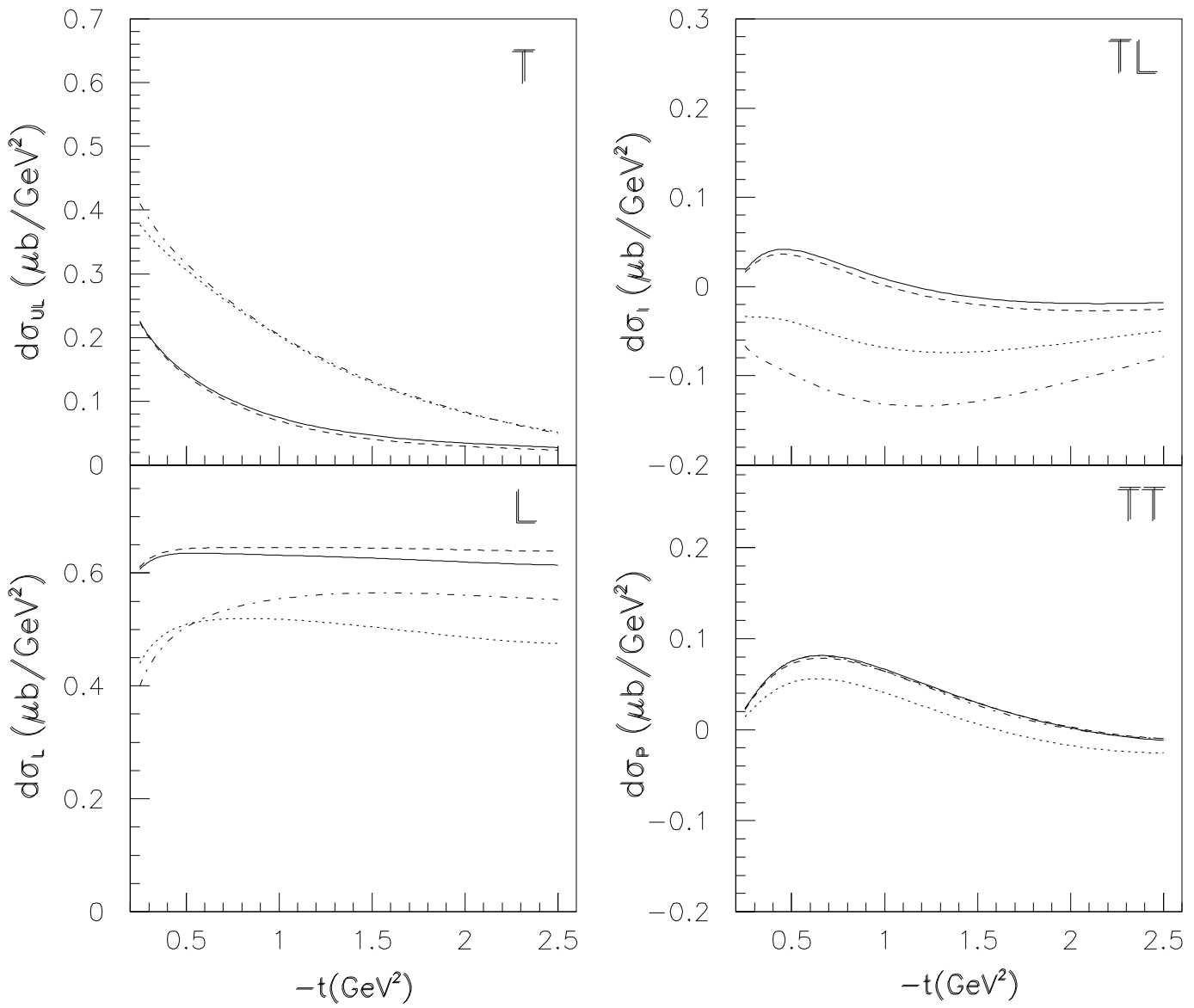
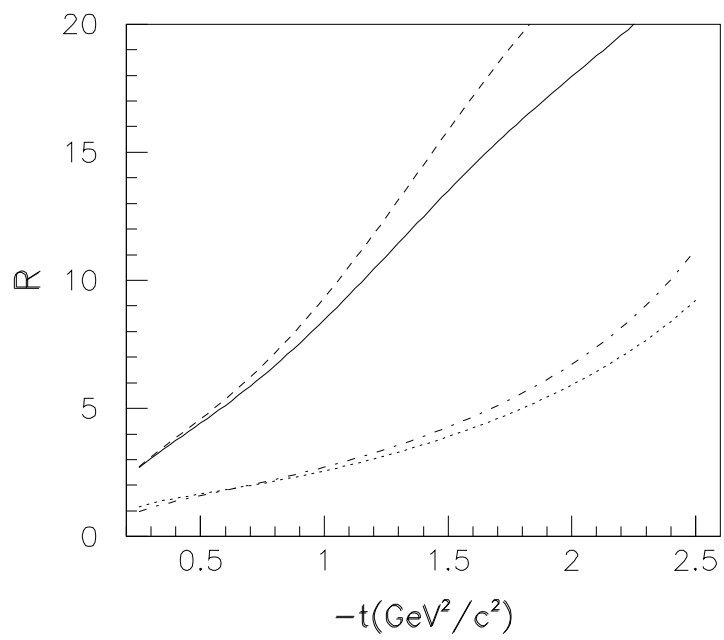


FIG. 6 - Mizutani et al., Off-shell effects...



**FIG. 7 - Mizutani et al., Off-shell effects...**

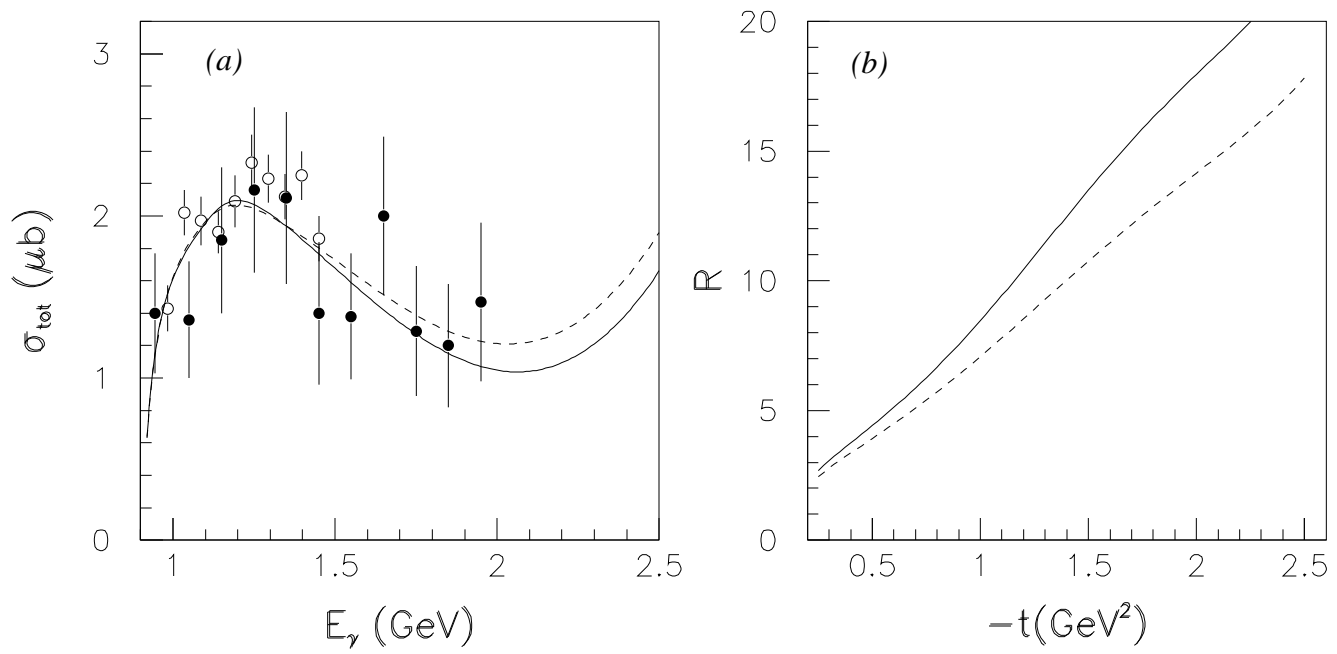


FIG. 8 - Mizutani et al., Off-shell effects...